223
363
544

Clarke, Modet & C°

COLOMB

SUPERINTENDENCIA DE INDUSTRIA Y COMERCIO
No. 05-044485- -00010-0000
Fecha: 2010-05-20 16:00:49 Dep. 2020 DIR.NUEVASCR
Tra. 11 PATENTEYII Eve: 379 FASENACIONALII
Act. 444 RESPUESTAREQUE Folios: 37

SUPERINTENDENCIA DE INDUSTRI
DIVISION DE NUEVAS CREACIONES
E. S. D.

Re: Expediente No. **05-044.485**
Solicitud de patente a nombre de **Independent Natural Resources, Inc.**

Yo, DILIA MARIA RODRIGUEZ D'ALEMAN, identificada como aparece al pie de mi firma, domiciliada en la Carrera 11 No. 86-53, piso 6, obrando como apoderada de la sociedad **Independent Natural Resources, Inc.**, domiciliada en Edina, Minnesota, Estados Unidos de América, solicitante de la patente de la referencia, en respuesta al oficio No. 2632 notificado por fijación en lista el 26 de febrero de 2010, me permito acompañar los siguientes documentos solicitados por ese despacho:

1. "DESIGN OPTIMIZATION OF AXIS-SYMMETRIC TAIL TUBE BUOYS" HYDRODYNAMICS OF OCEAN WAVE-ENERGY UTILIZATION. IUTAM SYMPOSIUM, 1985, pages 103-111, XP008003281.

2. "THE ABSORPTION OF WAVE ENERGY BY A THREE-DIMENSIONAL SUBMERGED DUCT", JOURNAL OF FLUID MECHANICS, CAMBRIDGE UNIVERSITY PRESS, CAMBRIDGE, GB, vol. 104, March 1981 (1981-03), pages 189-215, XP008003242 ISSN: 0022-1120.

Espero con esto haber dado cabal cumplimiento a lo solicitado por ese despacho y de conformidad con lo indicado en los artículos 3°, inciso 3, 35 inciso 2 y 59 inciso 2 del CCA, al analizar este memorial, atentamente solicito se traten todas las cuestiones planteadas con motivo del mismo.

Señor Superintendente,

DILIA MARIA RODRIGUEZ D'ALEMAN
CC. 41.654.882
TP 20824 CSJ
ADP

P-647

224
~~364~~
545

BEST AVAILABLE COPY

XP-008003281

P.D. 1985
P. 103-111 (9)

Design Optimization of Axi-symmetric Tail Tube Buoys

T.J.T. Whittaker, F.A. McPeake.

The Queen's University of Belfast,
Dept. of Civil Engineering,
David Keir Building,
Stranmillis Rd.,
Belfast, N. Ireland.

Summary

This paper presents the results of an experimental test programme and theoretical analysis of the hydrodynamic design of wave powered axi-symmetric navigation buoys. A two degree of freedom system with power extraction damping the relative motion of the two heave modes is considered. Results are presented for a theoretical model which has been verified experimentally.

It is concluded that the power extraction efficiency and frequency bandwidth of the current design of wave powered navigation buoy can be considerably improved. Peak capture factor increases proportionally with the tube diameter for tube / buoy diameter ratios of up to 75%. Increased tube length widens the frequency bandwidth response. The level of applied damping has considerable effect on peak performance and frequency bandwidth response. With this two degree of freedom system, the levels of applied damping which produce maximum capture factor are approximately 20 times greater than the optimum values for the isolated water columns. Also the radiation damping associated with the two heave modes should be similar so that the damping applied by the power extraction system is matched at both natural response frequencies. The work has general application to the design of wave powered buoys with a central cylindrical water column.

Notation

B	radiation dampng.
Ba	applied damping; (turbine damping.)
Bab	optimum applied damping at water column resonance.
C	damping ratio; Ba / Bab.
D	non dimensional radiation damping.
F	wave excitation force.
k	buoyancy.
L	tail tube length from water line.
Ma	added mass, (dynamic.)
Ms	mass, (static.)
R	buoy hull radius.
r	tail tube radius.
z	displacement from equilibrium position.
ρ	water density.
ω	frequency in radians.
Suffix b.	refers to the buoy hull.
Suffix w.	refers to the water column.

C-35

2

~~225~~
~~365~~
546

Introduction.

During the past few years, a research team based in The Department of Civil Engineering, The Queen's University of Belfast, have been investigating the various stages in the power conversion chain of wave powered navigation buoys. This work has been conducted jointly with two of the lighthouse authorities in the British Isles, Trinity house and Irish Lights, and a local company Munster Simms Engineering Ltd., who manufacture Wells turbine generators. Although the main thrust of the work has been towards the design and testing of Wells turbine-generators for use on standard tail tube buoys, as described by Whittaker et al (1), it has been necessary to gain a fundamental understanding of the hydrodynamic interaction between the buoy and the incident wave field.

The use of waves to power navigation buoys is not a recent innovation as they were first introduced in the early nineteenth century. These early systems used the rolling and pitching motions of the hull to sound a bell. Around the turn of the century the oscillating water column was introduced. A long cylindrical tube open to the sea at the bottom was located on the vertical centre line of the buoy forming a water column and air chamber above. A typical wave powered buoy as used by The Irish Lights Lighthouse Authority, is shown in figure 1. Air forced into and out of the plenum chamber by the wave induced oscillation of the water column was used to sound a whistle. The modern wave powered buoy utilises this same principle only the whistle is often replaced by a turbine generator. Masuda (2) describes such a system with a conventional axial flow turbine requiring complicated ducts and non-return valves to rectify the oscillating air flow to obtain uni-directional rotation. Whittaker et al (3) describes the use of the Wells self-rectifying turbine which has greatly simplifed the power conversion system.

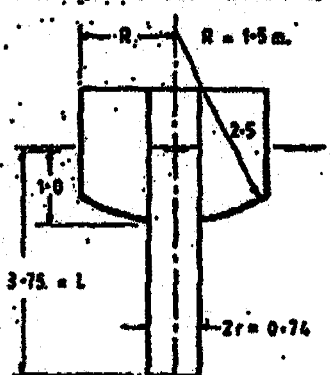

Fig. 1

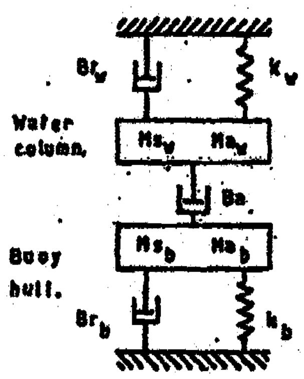

Fig. 2

Buoy hydrodynamics.

The buoy has a total of seven degrees of freedom; six to

~~226~~
~~366~~
547

describe the motion of the hull, plus the heave motion of the water column. The motion of the buoy hull in uni-directional waves can be described in terms of heave, pitch and surge. Calculation and model testing have shown that the natural pitch response frequency is outside the power extraction frequency bandwidth and surge motions are limited in this frequency range by a heavily damped mooring. Coupling between pitch and surge is minimal as a result of the mooring attachment on the bottom of the hull. Roll is not normally excited because of the bridal mooring which provides a two point attachment on the transverse axis of the hull. Air compliance in the plenum chamber was considered to be small and was not included in the mathematical model.

Therefore, the hydrodynamic model was limited to that of a two degree of freedom mass, spring, damper system, as shown in figure (2). One mode describes the heave motion of the buoy hull and the second is for the water column in the tail tube. The equation of motion for this model is presented in matrix form in equation 1.

$$\begin{bmatrix} Ms_b+Ma_b & Ma_{bw} \\ Ma_{wb} & Ms_w+Ma_w \end{bmatrix} \begin{bmatrix} -\omega^2 x_b \\ -\omega^2 x_w \end{bmatrix} + \begin{bmatrix} B_b+Ba & -Ba+B_{bw} \\ -Ba+B_{wb} & B_w+Ba \end{bmatrix} \begin{bmatrix} j\omega x_b \\ j\omega x_w \end{bmatrix} + \begin{bmatrix} K_b & 0 \\ 0 & K_w \end{bmatrix} \begin{bmatrix} x_b \\ x_w \end{bmatrix} = \begin{bmatrix} F_B \\ F_W \end{bmatrix} \qquad \text{Equation 1.}$$

The heave modes are coupled in two ways. Hydrodynamic coupling exists as indicated by the off-diagonial terms in the added mass and radiation damping matrices. However, the dominant coupling results from the damping applied by the turbine ot the air flow from the plenum chamber which damps the relative motion of the buoy hull and water column.

Test Programme.

The primary objective of the research programme was to determine how the length and diameter of the tail tube and the magnitude of the turbine damping affected the pneumatic power output from this type of device. This was accomplished by testing a range of buoy / tail tube configuratons in the wave tank and measuring the pneumatic performance with a range of applied damping levels. In addition the added mass and damping coefficients were calculated using a 3 D. diffraction theory program and the performance calculated by solving the equations of motion using the 'frequency response method'.

The hull shape, shown in figure 1, was chosen for these experiments as it represented one of the standard hull forms used by the lighthouse authorities throughout the world. A 1/10 scale was chosen for the models to suit the characteristics of the wave tank. Initially the complete Irish Lights buoy with a 3.75m. long, 0.74m. diameter tail tube was modelled as a control experiment to establish the performance of a typical buoy currently in service. This work was also used to design a Wells turbine generator with matched damping characteristics which was tested on a fully instrumented buoy

4

at sea as described by Whittaker et al (4).

Table 1 shows the full range of variables tested. For each tail tube geometric configuration, the applied damping is expressed in terms of damping ratio relative to the optimum applied damping for a fixed tail tube; optimum damping being defined as the value which produces peak pneumatic power output.

Tube diameters.	0.64		0.74		0.11	0.16		0.23
Tube lengths.	0.2		0.3		0.4			
Damping ratios.	1	5	10	15	20	30	40	50

The above values refer to model scale.

Table 1.

Validation of the Mathematical Model.

The performance curves predicted by the theoretical model for the range of buoy configurations shown in table 1. were checked experimentally. A sample of the calculated performance curves is compared with those obtained from the wave tank experiments in figure 3.

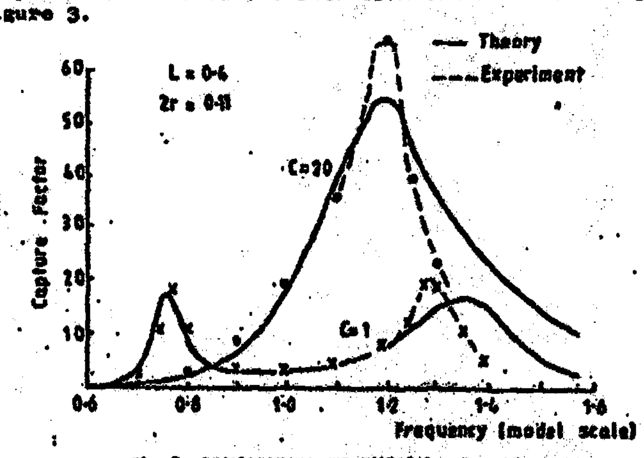

Fig. 3. COMPARISON OF THEORY – EXPERIMENT.

These curves relate capture factor to wave frequency at model scale for a range of applied damping. Capture factor is defined as the ratio of pneumatic power output to the wave power incident on the buoy diameter. The general trends of the curves are well modelled over most of the frequency range. However, some differences are evident at higher wave frequencies. This is a result of the experimental model being effectively in line array in the wave tank. As the wavelength is equal to the tank width at 1.33 Hz., array interaction enhances performance below this frequency and reduces performance beyond because of the phase of the radiated wave reflecting from the tank walls;

~~228~~
~~358~~
549

Whittaker (5). Array interaction was not included in the mathematical model as this phenomenon does not exist with isolated navigation buoys at sea. Therefore it was concluded that the calculated response was an accurate representation of the performance of a single buoy. The predictions of the mathematical model were also compared with results published by Evans (6) for a Norwegian buoy design. Excellent agreement was observed.

Performance of the Standard Buoy.

Before presenting the results of the parameter study it is necessary to discuss the performance of the standard Irish Lights buoy with a 0.74m. diameter 3.75m. long tail tube, as shown in figure 4.

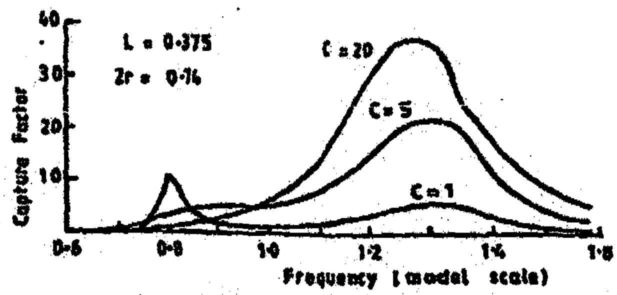

Fig. 4. IRISH LIGHTS WAVE POWERED BUOY.

Damping ratio significantly affects performance. A double peak performance curve identifying the heave resonant frequency of both the water column and buoy hull is only experienced with very light damping; a damping ratio of 1. However, the peak performance is only 30% of that obtained with a damping ratio of 20. At this higher damping level the water column resonance is completely suppressed resulting in a narrow frequency bandwidth response about the natural buoy heave frequency. The reason for this can be found by considering the magnitude of the radiation wave force components for both modes of motion, shown in figure 8. As there is a difference of nearly two orders of magnitude in the radiation damping, it is impossible to provide matched impedance for both modes with a single turbine design.

With the present buoy design the turbine damping is chosen to provide peak performance at the buoy heave frequency. This has the secondary effect of constraining the system to extract power only from low wave periods; typically 3 seconds at full scale. This period corresponds to a low spectral density in a typical sea spectrum even for an inshore location. It is therefore desirable to not only increase peak performance and bandwidth response but also to increase the response at larger wave periods and obtain a better matching between the transfer function for power extraction and the wave spectrum.

6

~~229~~
~~369~~
550

Tail-tube Geometry and Performance.

The effect of increasing tail tube diameter is shown in figure 5. for a 0.4m. long tube and for a damping ratio of 1. This shows that capture factor increases proportionally with water column area for the range of tubes tested. It should be noted that the lowest curve is similar to that obtained for the Irish Lights buoy with unit damping ratio.

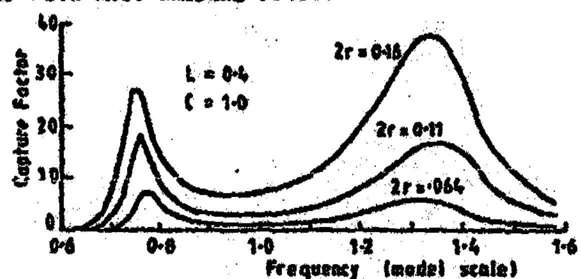

Fig. 5. VARIATION OF TUBE DIAMETER.

Figure 6. shows the effect of tail tube length on performance for unit damping ratio. Although the results for the intermediate diameter tube (0.11m.) are presented, the trend was similar for the other tubes. Lengthening the tail tube widened the response frequency band width as a consequence of the greater column mass lowering the stiffness / mass ratio and reducing the resonance frequency of the water column. The principal values of added mass and radiation damping varied insignificantly with tube length. However, a higher degree of hydrodynamic coupling was observed with the shorter columns, but this proved to be numerically insignificant when solving the equation of motion.

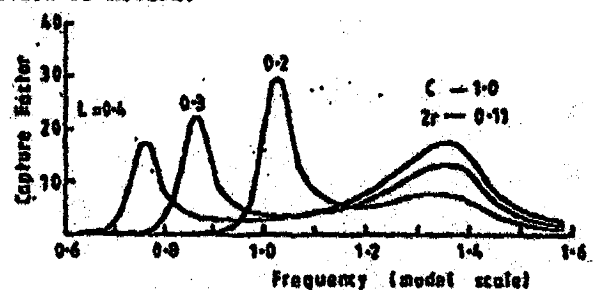

Fig. 6. VARIATION OF TUBE LENGTH.

As with the performance of the Irish Lights buoy damping proved to be the most significant variable irrespective of tube length or diameter. Figure 7. shows the performance of the 0.16m. diameter tube, with a range of damping levels. As with the standard buoy, increased damping ratio increased performance and a value was reached beyond which peak capture factor was

7

~~230~~
~~370~~
351

reduced. However, a comparative examination of figures 4 and 7 reveals that with the larger diameter tube the peak capture factor occurs at a frequency between the resonance frequency of the buoy hull and water column. Examination of the performance curves for all the column diameters tested, revealed that with a damping ratio of 20 the frequency corresponding to peak performance shifted to a lower value progressively with increasing tube diameter. This reduction in frequency is advantageous as it corresponds to a longer wave length providing beter matching with a typical inshore sea spectrum.

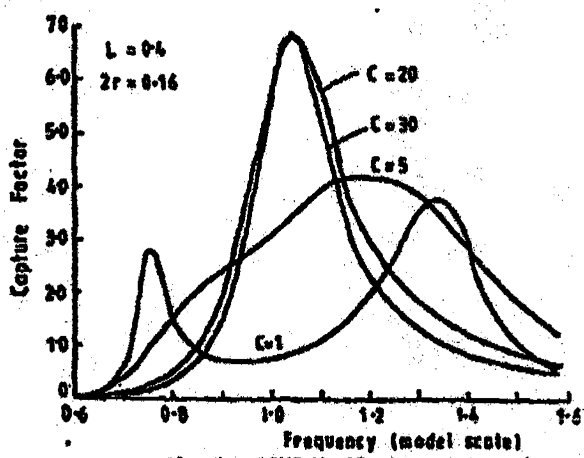

Fig. 7. VARIATION OF APPLIED DAMPING.

Optimum Buoy Design.

The standard navigation buoy represents one extreme in geometry when the water column cross sectional area is small in relation to that of the buoy hull. In this case the buoy heave mode predominates and the water column acts as an inertial reference for the power take-off. Wave excitation on the column is small compared to the pressure force in the plenum chamber. As the column diameter is increased, both the wave excitation force and the radiation force become greater until the water column motion predominates and the buoy hull becomes the inertial reference for the power take-off. Figure 8 shows the variation in radiation damping with increasing column diameter.

As the power take-off is not unique to each mode but acts as the coupling mechanism between the buoy and water column heave, impedance matching for both modes can only be achieved if the respective magnitudes of radiation damping are of similar magnitude. This can be achieved with the larger diameter tail tubes.

8

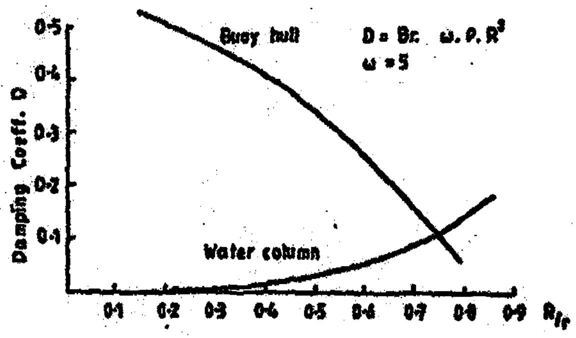

Fig.8. VARIATION OF RADIATION DAMPING COEFF.

However, it is not possible to optimise the buoy design purely from hydrodynamic considerations as there are practical limitations to the length and diameter of the tail tube. Diameter must be restricted to leave sufficient plane water area in the hull to ensure floatation. As navigation buoys are heavily constructed, this limits the column diameter to approximately half that of the hull. Column length is restricted by the depth of water on site and the mooring configuration. Buoys can be moored in a water depth of ten metres and as the mooring must be attached to the bottom of the hull for stability, a bridal must be used. With large diameter columns the length is limited to about 4m. to prevent contact with the mooring chains. The connection between the bridal and the main mooring chain at the swivel must not rest on the sea bed to avoid twisting. Column length must also be limited to enable handling of the buoy on the deck of the ship.

Conclusions

From the first stage of an extensive research and development programme to determine the relationship between water column geometry and the pneumatic performance of axi-symmetric tail tube buoys for use as navigation aids, the following has been concluded:-

1. Pneumatic performance is proportional to column cross sectional area for tube / diameter ratios of up to 75%.

2. Increased tube length widens the frequency bandwidth response by reducing the natural column heave frequency. This is most significant with low damping ratios.

3. The level of applied damping is the most significant variable affecting performance. For small diameter tubes, as used in the current buoy designs, a change in damping ratio from 1 to 20 increases the peak performance by a factor of three and the buoy heave frequency predominates.

4. As the power extraction damps the relative motion of the two heave modes, matched impedance necessitates similar levels of radiation damping for both degrees of freedom.

232
372
553

5. The current wave powered navigation buoy designs are not efficient and respond only to very high wave frequencies. Doubling the tube diameter not only improves peak performance while reducing the response frequency, but also substanially widens the frequency bandwidth response when a damping ratio of 20 is used.

6. Although hydrodynamic performance improves with increased water column diameter and length, for the range of variables tested, full optimisation is not possible as there are practical limitations such as floatation, stability, handling, water depth and snaging between the tube and the bridal mooring.

Acknowledgements

Grateful thanks are accorded to the following:-

The Wolfson foundation for funding the research work.

Dr. E R Jeffreys for his considerable assistance with the mathematical modelling and calculation of the hydrodynamic coefficients.

The academic and technical staff of the University and the members of the wave power research team for their considerable efforts in the development of this project.

References

1. Whittaker, T.J.T., McPeake,F.A., Barr,A.G., The Development and Testing of a Wave Activated Navigation Buoy with a Wells Turbine. 3rd Int. Symp. on Offshore Mechanics and Engineering, New Orleans, LA, USA, Feb. 12-16, 1984, pp 267-273, Vol 2.

2. Masuda,Y. Wave Activated Generator. Int. Coll. on the Exploitation of the Oceans. (Trans.), Bordeaux, France 1971.

3. Whittaker,T.J.T., McIlhagger,D.S., Barr,A.G., Wells Turbines for Navigation Buoys. 3rd. Int. Conf. Energy for Rural and Island Communities. Inverness, Scotland Sept. 12-16, 1983, pp 289-297.

4. Whittaker,T.J.T., McIlhagger,D.S., Barr,A.G., THompson,A., Electrical Considerations with Wave Powered Navigation Aids Conf. Alternative Energy Systems: Elect. Integration and Utilisation. Coventry, U.K. Sept. 10-12.

5. Whittaker,T.J.T., Murray,M.A., Performance Characteristics of Hydropneumatic Buoys in Line Array. Proc. Int. Symp. on Hydrodynamics, Ocean Eng., Trondheim, 1981, pp 1047-1066.

6. Evans,D.V., McIver,P., The Hydrodynamical Characteristics of a Section of a Floating Sphere Making Vertical Oscillations. School of Mathematics University of Bristol: Report AM-82-09

10

554 ~~233~~
373

BEST AVAILABLE COPY

XP-008003242

P.D. 00-03-1981
p. 189-215 = (27)

J. Fluid Mech. (1981), vol. 104, pp. 189-215
Printed in Great Britain

The absorption of wave energy by a three-dimensional submerged duct

By J. R. THOMAS

School of Mathematics, University of Bristol, University Walk, Bristol BS8 1TW

(Received 20 May 1980)

It has been shown (Evans 1976) that the power absorbed by a general, axisymmetric body depends solely upon the added-mass and damping coefficients. These coefficients are fundamental properties of the body, representing the component of the force on the body proportional to the acceleration and velocity of the body respectively in the radiation problem, where the body is forced to oscillate in the absence of incoming waves.

In the present paper these coefficients are determined by solution of the radiation problem, for a mouth-upward cylindrical duct situated on the sea bed and fitted with a piston undergoing forced oscillations. The added-mass and damping coefficients are then used to study the power absorption properties of the duct when the power take-off is modelled by a linear-spring-dashpot system attached to the piston. Curves of the added mass, damping coefficients and absorption length (a measure of the power absorbed) as functions of wavenumber are presented, for different duct diameters and different depths of submergence.

1. Introduction

One type of wave-energy absorber under current consideration is the submerged device situated on the sea bed. Although moving away from the sea surface towards the sea bed will, in general, tend to narrow the absorption length† *vs.* wavenumber bandwidth of the device, it has the advantage of shielding the absorber, to some extent, from local storms which could cause damage to a surface device.

Mouth-upward-facing ducts in two dimensions have been studied by Lighthill (1979) using complex analysis to obtain the various important hydrodynamic coefficients. Later work by Simon (1981) extends this to three dimensions, where use is made of reciprocal relations which exist between the scattering and radiation problems in the linear theory, together with an approximate variational technique.

In this paper, we shall consider the three-dimensional case of an upward-facing duct of circular cross-section, fitted with a piston, at sea-bed level for mathematical simplicity, which is attached to a spring-dashpot system as a means of extracting energy. Simon uses a similar model, although he treats the infinite depth case where the power take-off system is now modelled by an energy extraction coefficient (equivalent to a dashpot) applied in the depths of the duct.

Evans (1976) has shown that the absorption length may be determined from

† Absorption length = the ratio of energy absorbed by the device to the energy per unit frontage of incident wave.

7-2

C-34

11

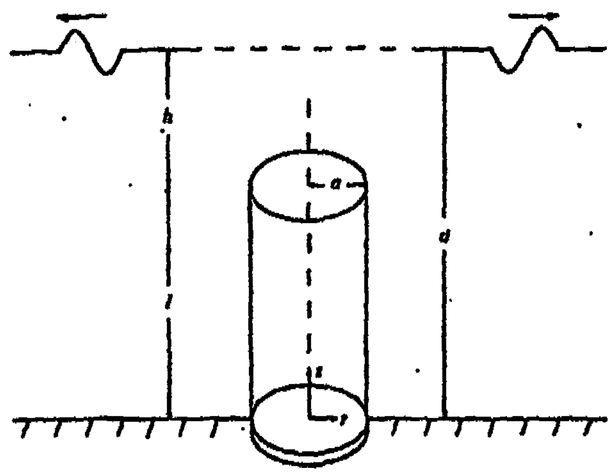

FIGURE 1. Mouth-upward duct of radius a, length l, in water of depth d.

knowledge of fundamental properties of the absorbing body: the added-mass and damping coefficients. Waves incident upon the device will be diffracted, scattering in all directions, and will also set the piston in motion, generating further waves. As explained fully in Newman (1977) the velocity potential can thus be decomposed into scattering potential, where the piston is held fixed in the presence of incoming waves, and a radiation potential, where the piston is forced to oscillate with unit amplitude in the absence of incoming waves. The added-mass and damping coefficients may be obtained by evaluating the hydrodynamic force on the piston in the radiation problem.

Hence, to study the absorption length we need only consider the problem of forced oscillations of the piston. The method of solution relies on finite depth and is due to Garrett, who considered the problems of bottomless harbours (1970) and the wave forces on a circular dock (1971).

Added-mass and damping curves as functions of wavenumber are given in §6. For narrow tubes the added-mass coefficient remains fairly constant over the range considered, being in general slightly larger than the mass of water in the tube. As the tube length increases, it is shown that the absorption-length bandwidth decreases at first before reaching a minimum and increases again as the mouth of the duct approaches the surface. It appears that the main advantage of the tube is that it reduces the piston motion as the tube length increases. A comparison of these coefficients is made with those obtained by Simon (1981) in infinite depth.

The limiting case of an oscillating disk on the sea bed is considered in §5. This is easily solved and provides a useful check on the computation necessary in the above case.

In appendix B the absorption length and amplitude ratio in finite depth are derived for a general axisymmetric heaving body. In the limiting case of infinite depth the expressions agree with those obtained by Evans (1976) and, as in the infinite depth case, the maximum absorption length obtainable by an axisymmetric heaving body is $\lambda/2\pi$, where λ is the wavelength of the incoming waves which is now dependent on the water depth.

12

356 ~~235~~ ~~375~~

2. Formulation

The radiation problem

A submerged vertical tube of length l and circular cross-section of radius a stands on the sea bed in water of depth d ($d > l$). The tube is fitted with a piston, which is forced to oscillate with frequency ω and unit amplitude. We wish to find the hydrodynamic force on the piston and hence the added-mass and damping coefficients of the device.

Cylindrical polar co-ordinates (r, θ, z) are used with z positive upwards and the origin at the mean position of the centre of the piston (figure 1).

Assuming small displacements and irrotational flow, the fluid motion is governed by classical linearized water-wave theory. There is no θ dependence in the problem by symmetry, so we may introduce a velocity potential,

$$\Phi(r, z, t) = \mathrm{Re}\{\phi(r, z)\, e^{-i\omega t}\}, \tag{2.1}$$

where, following the usual convention, the time co-ordinate is suppressed. The potential ϕ must satisfy

$$\nabla^2\phi = \frac{\partial^2\phi}{\partial r^2} + \frac{1}{r}\frac{\partial\phi}{\partial r} + \frac{\partial^2\phi}{\partial z^2} = 0 \quad \text{in the fluid,} \tag{2.2}$$

with the linearized boundary conditions

$$K\phi - \frac{\partial\phi}{\partial z} = 0 \quad \text{on the free surface} \quad (z = d), \tag{2.3}$$

where $K = \omega^2/g$,

$$\frac{\partial\phi}{\partial z} = 1 \quad \text{on the piston} \quad (z = 0, \quad r < a), \tag{2.4}$$

$$\frac{\partial\phi}{\partial z} = 0 \quad \text{on the sea bed} \quad (z = 0, \quad r > a), \tag{2.5}$$

$$\frac{\partial\phi}{\partial r} = 0 \quad \text{on the tube} \quad (r = a, \quad 0 \leqslant z \leqslant l). \tag{2.6}$$

We also require ϕ to satisfy the appropriate radiation condition,

$$\phi \sim \frac{\mathscr{A} e^{ikr}}{(kr)^{\frac{1}{2}}} \frac{\cosh kz}{\cosh kd} \quad \text{as} \quad r \to \infty, \tag{2.7}$$

where $\mathscr{A}$ is some constant.

We may solve Laplace's equation in the inner ($r \leqslant a$) and outer ($r \geqslant a$) regions, giving

$$\phi = \sum_{n=0}^{\infty} B_n K_0(\alpha_n r) Z_n(z) \quad (r \geqslant a), \tag{2.8}$$

$$\phi = \sum_{n=0}^{\infty} A_n I_0(\alpha_n r) Z_n(z) + [(z-d) + g/\omega^2] \quad (r \leqslant a), \tag{2.9}$$

where A_n, B_n are unknown constants and, in the notation of Miles & Gilbert (1968),

$$Z_0(z) = N_0^{-\frac{1}{2}} \cosh kz, \quad \text{where} \quad N_0 = \tfrac{1}{2}[1 + (2kd)^{-1} \sinh 2kd], \tag{2.10}$$

$$Z_n(z) = N_n^{-\frac{1}{2}} \cos \alpha_n z, \quad \text{where} \quad N_n = \tfrac{1}{2}[1 + (2\alpha_n d)^{-1} \sin 2\alpha_n d], \tag{2.11}$$

for $n \geqslant 1$.

13

236
376
557

Here k is the wavenumber related to ω through the dispersion relation

$$\omega^2 = gk \tanh kd \quad (\text{also given by} \quad \alpha_0 = -ik), \tag{2.12}$$

and α_n are the positive real roots of

$$g\alpha \tan \alpha d = -\omega^2, \tag{2.13}$$

with $\alpha_n < \alpha_{n+1}$ ($n \geqslant 1$).

The $Z_n(z)$ ($n \geqslant 0$) form a complete orthogonal set in $[0, d]$ with mean-square values of 1.

Note that

$$K_0(-ikr) = \tfrac{1}{2}\pi i H_0(kr), \tag{2.14}$$

$$I_0(-ikr) = J_0(kr), \tag{2.15}$$

where J_0 is an ordinary Bessel function, I_0 and K_0 are modified Bessel functions and H_0 is the zero-order Hankel function of the first kind (the usual superscript may be omitted without ambiguity as a result of the radiation condition).

As in Black, Mei & Bray (1971), we have included a particular solution in the inner region, which is harmonic and satisfies conditions (2.3) and (2.4).

Following Miles & Gilbert (1968) we now construct ϕ in the inner and outer regions in terms of $\partial\phi/\partial r$ at the cylindrical interface $r = a$, $l \leqslant z \leqslant d$.

Suppose

$$\frac{\partial \phi}{\partial r} = f(z) \quad \text{at} \quad r = a, \quad l \leqslant z \leqslant d, \tag{2.16}$$

we have also

$$\frac{\partial \phi}{\partial r} = 0 \quad \text{at} \quad r = a, \quad 0 \leqslant z \leqslant l. \tag{2.17}$$

Hence we may expand $\partial\phi/\partial r$ over $0 \leqslant z \leqslant d$ as

$$\left.\frac{\partial \phi}{\partial r}\right|_{r=a} = f(z) = \sum_{n=0}^{\infty} \mathscr{F}_n Z_n(z), \tag{2.18}$$

where

$$\mathscr{F}_n = \frac{1}{d}\int_l^d f(z)\, Z_n(z)\, dz. \tag{2.19}$$

The representations of ϕ in the inner and outer regions now become

$$\phi = \sum_{n=0}^{\infty} \frac{\mathscr{F}_n K_0(\alpha_n r)}{\alpha_n K_0'(\alpha_n a)} Z_n(z) \quad (r \geqslant a), \tag{2.20}$$

$$\phi = \sum_{n=0}^{\infty} \frac{\mathscr{F}_n I_0(\alpha_n r)}{\alpha_n I_0'(\alpha_n a)} Z_n(z) + \left[(z-d) + \frac{g}{\omega^2}\right] \quad (r \leqslant a). \tag{2.21}$$

The pressure, and hence ϕ, is continuous at $r = a$, $l \leqslant z \leqslant d$, so matching the solution in the inner and outer regions gives

$$\sum_{n=0}^{\infty} \mathscr{F}_n \left\{\frac{K_0(\alpha_n a)}{\alpha_n K_0'(\alpha_n a)} - \frac{I_0(\alpha_n a)}{\alpha_n I_0'(\alpha_n a)}\right\} = (z-d) + \frac{g}{\omega^2} \tag{2.22}$$

valid for $l \leqslant z \leqslant d$.

This may be simplified using the formula (Abramowitz & Stegun 1970)

$$-I_0(\alpha_n a) K_0'(\alpha_n a) + I_0'(\alpha_n a) K_0(\alpha_n a) = (\alpha_n a)^{-1} \quad \text{for} \quad n \geqslant 0. \tag{2.23}$$

~~237~~
~~377~~
558

Define

$$R_n = -[\alpha_n^2 a^2 I_0'(\alpha_n a) K_0'(\alpha_n a)]^{-1} \quad \text{for} \quad n \geqslant 0, \tag{2.24}$$

and equation (2.22) then becomes

$$\sum_{n=0}^{\infty} \mathscr{F}_n R_n Z_n(z) = \frac{1}{a}[(d-z) - g/\omega^2], \quad l \leqslant z \leqslant d. \tag{2.25}$$

3. Solution

Miles & Gilbert proceeded to set up an integral equation; however we shall adopt the approach of Garrett and construct an infinite system of simultaneous linear equations for the unknown $\mathscr{F}_n$.

Over $0 \leqslant z \leqslant l$ we have, from equation (2.6)

$$\sum_{n=0}^{\infty} \mathscr{F}_n Z_n(z) = 0. \tag{3.1}$$

Multiply (2.25) and (3.1) by $Z_m(z)$, integrate over region of validity, divide by d and add. Thus

$$\sum_{n=0}^{\infty} E_{mn} \mathscr{F}_n = C_m, \tag{3.2}$$

where

$$E_{mn} = (R_n - 1) D_{mn} + \delta_{mn}, \tag{3.3}$$

$$D_{mn} = \frac{1}{d}\int_l^d Z_m(z) Z_n(z)\, dz \tag{3.4}$$

and

$$C_m = \frac{1}{ad}\int_l^d [(d-z) - g/\omega^2] Z_m(z)\, dz \tag{3.5}$$

(see appendix A for expressions for D_{mn}, C_m).

The above is a complex matrix equation which can be reduced to two real matrix equations, more easily solved by the computer, by writing

$$\mathscr{F}_n = a_n + ib_n, \tag{3.6}$$

where a_n, b_n are real, and uncoupling the resulting equation (see Ogilvie 1963).

Note that E_{mn} is real except for $n = 0$ (since $R_0 = -[\tfrac{1}{2}\pi i k^2 a^2 J_0'(ka) H_0'(ka)]^{-1}$). Writing

$$E_{m0} = \gamma_m + i\beta_m \quad (m \geqslant 0), \tag{3.7}$$

where γ_m, β_m are real (see appendix A for expressions for γ_m, β_m), then from (3.2) we have

$$\sum_{n=1}^{\infty} E_{mn}(a_n + ib_n) + (\gamma_m + i\beta_m)(a_0 + ib_0) = C_m. \tag{3.8}$$

Equate real and imaginary parts to obtain

$$\sum_{n=1}^{\infty} E_{mn} a_n + \gamma_m a_0 = C_m + b_0 \beta_m, \tag{3.9}$$

$$\sum_{n=1}^{\infty} E_{mn} b_n + \gamma_m b_0 = -a_0 \beta_m. \tag{3.10}$$

15

If ϵ_n, δ_n are the solutions of

$$\gamma_m \epsilon_0 + \sum_{n=1}^{\infty} E_{mn} \epsilon_n = C_m, \tag{3.11}$$

$$\gamma_m \delta_0 + \sum_{n=1}^{\infty} E_{mn} \delta_n = \beta_m, \quad m = 0, 1, 2, \ldots, \tag{3.12}$$

then

$$a_n = \epsilon_n + b_0 \delta_n, \tag{3.13}$$

$$b_n = -a_0 \delta_n, \quad n = 0, 1, 2, \ldots, \tag{3.14}$$

and, in particular,

$$a_0 = \epsilon_0 + b_0 \delta_0, \quad b_0 = -a_0 \delta_0. \tag{3.15}$$

Thus

$$a_0 = \frac{\epsilon_0}{1+\delta_0^2}, \quad b_0 = -\frac{\epsilon_0 \delta_0}{1+\delta_0^2}, \tag{3.16}$$

and

$$\begin{aligned} \mathscr{F}_n &= a_n + ib_n \\ &= \left\{\epsilon_n - \frac{\epsilon_0 \delta_0 \delta_n}{1+\delta_0^2}\right\} + i\left\{-\frac{\epsilon_0 \delta_n}{1+\delta_0^2}\right\}, \quad n \geqslant 0. \end{aligned} \tag{3.17}$$

So, upon solving the two real systems of equations (3.11), (3.12) (the method employed is given in §6.3), we can evaluate $\mathscr{F}_n (n \geqslant 0)$ and obtain a full solution for ϕ from equations (2.20), (2.21).

4. Calculation of added-mass and damping coefficients and energy extraction

4.1. *Added-mass and damping coefficients*

It is shown in Newman (1977) that the complex force in the ith direction due to a sinusoidal motion of frequency ω and unit amplitude in the jth direction may be written in the form

$$f_{ij} = \omega^2 a_{ij} + i\omega b_{ij}, \tag{4.1}$$

where a_{ij}, b_{ij} are the added-mass and damping coefficients respectively, both real and dependent on frequency ω. It is also shown that by integrating the pressure over the body surface, $\mathscr{S}_B$,

$$f_{ij} = \rho \int_{\mathscr{S}_B} \frac{\partial \phi_i}{\partial n} \phi_j \, dS, \tag{4.2}$$

where ϕ_i is the potential corresponding to motion in the ith direction and n is the unit normal vector on the body surface, directed into the fluid.

In this case the only moveable part of the body is the piston, which is restricted to motion in the z direction; hence only a_{33}, b_{33} are non-zero and

$$f_{33} = \omega^2 a_{33} + i\omega b_{33} \tag{4.3}$$

$$= \rho \int_{\mathscr{S}} \frac{\partial \phi_3}{\partial z} \phi_3 \, dS, \tag{4.4}$$

where $\mathscr{S}$ is the piston surface. (For convenience, a_{33}, b_{33} will hereafter be denoted by a_3, b_3.)

~~239~~
~~379~~
560

Since the motion is of unit amplitude we require

$$\frac{\partial \phi_3}{\partial z} = -i\omega \quad \text{on } \mathscr{S}, \tag{4.5}$$

and thus ϕ_3 is related to the potential ϕ defined in §2 in the following way,

$$\phi_3 = -i\omega\phi \tag{4.6}$$

using (2.4).

Hence

$$\omega^2 a_3 + i\omega b_3 = -\rho\omega^2 \int_{\mathscr{S}} \phi \, dS. \tag{4.7}$$

Using the representation of ϕ in the inner region (2.21),

$$\omega^2 a_3 + i\omega b_3 = -\rho\omega^2 \int_{r=0}^{a} \int_{\theta=0}^{2\pi} \left[(g/\omega^2 - d) + \sum_{n=0}^{\infty} \frac{\mathscr{F}_n I_0(\alpha_n r)}{\alpha_n I_0'(\alpha_n a)} Z_n(0) \right] r \, dr \, d\theta \tag{4.8}$$

$$= -2\pi\rho\omega^2 \left[(g/\omega^2 - d) \int_0^a r \, dr + \sum_{n=0}^{\infty} \frac{\mathscr{F}_n N_n^{-\frac{1}{2}}}{\alpha_n I_0'(\alpha_n a)} \int_0^a I_0(\alpha_n r) \, r \, dr \right. \tag{4.9}$$

$$= -2\pi\rho\omega^2 \left[(g/\omega^2 - d)\frac{a^2}{2} + \sum_{n=0}^{\infty} \frac{a N_n^{-\frac{1}{2}} \mathscr{F}_n}{\alpha_n^2} \right]. \tag{4.10}$$

Thus

$$a_3 = 2\pi\rho \left[(d - g/\omega^2)\frac{a^2}{2} + \operatorname{Re} \sum_{n=0}^{\infty} \frac{a N_n^{-\frac{1}{2}} \mathscr{F}_n}{\alpha_n^2} \right], \tag{4.11}$$

$$b_3 = -2\pi\rho\omega \left[\operatorname{Im} \sum_{n=0}^{\infty} \frac{a N_n^{-\frac{1}{2}} \mathscr{F}_n}{\alpha_n^2} \right]. \tag{4.12}$$

4.2. *Absorption length and amplitude ratio*

The power absorption length is defined by

$$l_d = \frac{\text{power absorbed by body}}{\text{total power in incident wave of unit frontage}},$$

and it can be shown that for the finite depth case (see appendix B)

$$l_d = \frac{4(\omega^2/k)\, b_3 \bar{d}}{(\bar{k} - a_3\omega^2)^2 + \omega^2(b_3 + \bar{d})^2}, \tag{4.13}$$

for a light piston with spring and damper constants $\bar{k}$, $\bar{d}$ respectively. Now l_d may be rewritten as

$$l_d = \frac{1}{k}\left\{1 - \frac{(\bar{k} - a_3\omega^2)^2 + \omega^2(\bar{d} - b_3)^2}{(\bar{k} - a_3\omega^2)^2 + \omega^2(\bar{d} + b_3)^2}\right\}, \tag{4.14}$$

giving a maximum value of

$$l_{d\max} = \frac{1}{k} = \frac{\lambda}{2\pi}, \tag{4.15}$$

where λ is the wavelength of the incident wave, when

$$\bar{k} = a_3\omega^2, \quad \bar{d} = b_3. \tag{4.16}$$

The result (4.15) agrees with the infinite depth case (Evans 1976).

17

Similarly the expression for the ratio of the piston amplitude ξ to the amplitude of the incident wave A, can be shown to be

$$\left|\frac{\xi}{A}\right|^2 = \frac{4\rho c_g b_3}{k[(\bar{k}-a_3\omega^2)^2+\omega^2(b_3+\bar{d})^2]}, \tag{4.17}$$

which again agrees with the deep water case as $d \to \infty$, when the group velocity $c_g \to g/2\omega$.

Before computing values of the added mass and damping we non-dimensionalize by

$$a_3 = M\mu, \quad b_3 = M\omega\lambda, \tag{4.18}$$

where

M = mass of water above piston contained in a cylinder of radius a
$= \pi a^2 \rho d$,

choosing this particular M instead of the mass of water in the tube so that we are able to consider the limiting case as the length of the tube tends to zero.

If we introduce a non-dimensional wavenumber $\nu = \omega^2 d/g$, then

$$\mu = 1 - \frac{1}{\nu} - 2\left(\frac{d}{a}\right)\left[\operatorname{Re}\sum_{n=0}^{\infty}\frac{N_n^{-\frac{1}{2}}\mathscr{F}_n}{(\alpha_n d)^2}\right], \tag{4.19}$$

$$\lambda = -2\left(\frac{d}{a}\right)\left[\operatorname{Im}\sum_{n=0}^{\infty}\frac{N_n^{-\frac{1}{2}}\mathscr{F}_n}{(\alpha_n d)^2}\right]. \tag{4.20}$$

Further, we may 'tune' the system to a frequency ω_0 to give l_a a maximum at this frequency, by assuming we may choose

$$\bar{k} = a_3(\omega_0)\,\omega_0^2, \quad \bar{d} = b_3(\omega_0). \tag{4.21}$$

Then we have

$$\frac{l_a}{2a} = \frac{1}{2ka}\,\frac{4\nu(\nu^{\frac{1}{2}}\lambda)(\nu_0^{\frac{1}{2}}\lambda_0)}{[(\mu_0\nu_0-\mu\nu)^2+\nu(\nu_0^{\frac{1}{2}}\lambda_0+\nu^{\frac{1}{2}}\lambda)^2]}, \tag{4.22}$$

$$\left|\frac{\xi}{A}\right|^2 = \frac{\left(\frac{2\lambda}{\pi\nu}\right)\left(\frac{d}{a}\right)^2(\tanh kd + kd\operatorname{sech}^2 kd)}{[(\mu_0\nu_0-\mu\nu)^2+\nu(\nu_0^{\frac{1}{2}}\lambda_0+\nu^{\frac{1}{2}}\lambda)^2]}, \tag{4.23}$$

where $\nu_0 = \omega_0^2 d/g$, $\mu_0 = \mu(\omega_0)$, $\lambda_0 = \lambda(\omega_0)$.

So, for each value of the non-dimensional wavenumber ν, we solve the two real linear systems of equations given by (3.11), (3.12) to evaluate $\mathscr{F}_n$ $(n \geqslant 0)$ and hence μ and λ. Once the variation of μ and λ with ν is known, and a tuning frequency ω_0 is chosen we can use (4.22), (4.23) to study the absorption length and amplitude ratio variation with ν.

The results obtained are presented and discussed in § 6. But first we shall examine the limiting case of an oscillating disk in some detail. It is not a practical absorber but the problem can be easily solved and the behaviour of the added-mass and damping coefficients studied.

~~241~~ ~~384~~ 562

5. Limiting disk case

5.1. *Statement of problem and solution*

An interesting limiting case of the resonant tube is that of an oscillating disk on the sea bed. The approach to the problem is as for the tube, but the fact that we are now matching ϕ at $r = a$ over the whole interval $[0, d]$ produces much simplified results providing a better insight into the behaviour of the added-mass and damping coefficients (the similar curves produced in the disk and tube cases indicate that this behaviour is relevant to the tube problem).

The formulation of the problem is clearly identical with that of the tube case, giving now, instead of (2.25)

$$\sum_{n=0}^{\infty} \mathscr{F}_n R_n Z_n(z) = [(d-g/\omega^2) - z]/a \quad \text{holding for} \quad 0 \leqslant z \leqslant d. \tag{5.1}$$

As before, multiply both sides by $(1/d)\, Z_m(z)$ and integrate to obtain

$$\mathscr{F}_m R_m = \frac{1}{ad}\int_0^d [(d-g/\omega^2)-z]\, Z_m(z)\, dz \tag{5.2}$$

$$= C_m \quad \text{with} \quad l = 0. \tag{5.3}$$

Thus

$$\mathscr{F}_0 = \frac{C_0}{R_0}, \quad \text{where} \quad C_0 = -\frac{N_0^{-\frac{1}{2}}}{k^2 ad} \quad \text{(see appendix A)}, \tag{5.4}$$

$$\mathscr{F}_m = \frac{C_m}{R_m} \quad (m \geqslant 1) \quad \text{where} \quad C_m = \frac{N_m^{-\frac{1}{2}}}{\alpha_m^2 ad} \quad \text{(see appendix A)}. \tag{5.5}$$

Hence

$$\mathscr{F}_0 = \frac{-N_0^{-\frac{1}{2}}}{k^2 ad}\left[-\tfrac{1}{2}\pi i k^2 a^2 J_0'(ka)\, H_0'(ka)\right] \tag{5.6}$$

$$= \frac{N_0^{-\frac{1}{2}}\pi}{2}\left(\frac{a}{d}\right)\left[-J_1(ka)Y_1(ka) + iJ_1^2(ka)\right], \tag{5.7}$$

since $H_0(ka) = J_0(ka) + iY_0(ka)$, and

$$\mathscr{F}_m = \frac{N_m^{-\frac{1}{2}}}{\alpha_m^2 ad}\left[-\alpha_m^2 a^2 I_0'(\alpha_m a)\, K_0'(\alpha_m a)\right] \tag{5.8}$$

$$= N_m^{-\frac{1}{2}}\left(\frac{a}{d}\right) I_1(\alpha_m a)\, K_1(\alpha_m a) \quad (m \geqslant 1). \tag{5.9}$$

5.2. *Added-mass and damping coefficients*

Using (4.11), (4.12) and the fact that the $\mathscr{F}_m$ are real for $m \geqslant 1$,

$$b_3 = 2\pi\rho\omega a N_0^{-\frac{1}{2}}\, \mathrm{Im}\,(\mathscr{F}_0/k^2), \tag{5.10}$$

$$a_3 = 2\pi\rho\left[(d-g/\omega^2)\frac{a^2}{2} - \mathrm{Re}\left(a\sum_{n=0}^{\infty}\frac{N_n^{-\frac{1}{2}}}{\alpha_n^2}\mathscr{F}_n\right)\right], \tag{5.11}$$

19

563 ~~248~~ 382

giving

$$b_3 = \frac{\pi^2 a^2 \rho\omega}{k^2 d} N_0^{-1} J_1^2(ka), \tag{5.12}$$

$$a_3 = \pi a^2 \rho \left[(d - g/\omega^2) - \frac{N_0^{-1}\pi}{k^2 d} J_1(ka) Y_1(ka) - \frac{2}{d} \sum_{n=1}^{\infty} \frac{N_n^{-1} I_1(\alpha_n a) K_1(\alpha_n a)}{\alpha_n^2} \right]. \tag{5.13}$$

I am indebted to a referee for pointing out that this problem of an oscillating disk may also be solved using a Hankel transformation. This method yields an expression for the damping coefficient identical to (5.12) and the following expression for the added-mass coefficient,

$$a_3 = -2\pi\rho a^2 \int_0^{\infty} \frac{J_1^2(\xi a)(\xi \cosh \xi d - K \sinh \xi d)}{\xi^3 (K \cosh \xi d - \xi \sinh \xi d)} d\xi, \tag{5.14}$$

where the integral is to be interpreted in the sense of the Cauchy principal value. By a suitable choice of contour the integral may be evaluated, giving an expression for the added-mass coefficient identical to (5.13).

We may now non-dimensionalize the result in exactly the same way as in the duct case and compute the absorption width and amplitude ratio variation with wave-number for the disk.

One point to note is that for frequencies where ka is equal to a zero of J_1 we have $b_3 = 0$ and, since (see appendix B) the damping coefficient is proportional to the far-field amplitude, we may conclude that, for an infinite set of frequencies, forced oscillation of the piston produces no outward-propagating waves. This is in accordance with the results of Black, Mei & Bray (1971) where they considered water-wave radiation by rigid oscillating bodies. However, the first zero of $J_1(ka)$ occurs at $ka = 3{\cdot}83171$, i.e.

$$\frac{2\pi d}{\lambda} \simeq 4\left(\frac{d}{a}\right) \quad \text{or} \quad \frac{\lambda}{d} \simeq \frac{2\pi}{4}\left(\frac{a}{d}\right).$$

So, assuming the water depth is 40–50 m, then, even when the diameter of the disk is equal to the water depth, the first zero will occur at a wavelength of the order of 30–40 m, which is outside the region of interest for wave-energy devices since the important energy source lies in waves of wavelengths between 100 and 200 m.

5.3. *Behaviour of coefficients as $\nu \to 0$, $\nu \to \infty$*

After non-dimensionalization,

$$\lambda = \frac{N_0^{-1} \pi J_1^2(ka)}{(kd)^2}, \tag{5.15}$$

$$\mu = 1 - \frac{1}{\nu} - \frac{N_0^{-1}\pi}{(kd)^2} J_1(ka) Y_1(ka) - 2 \sum_{n=1}^{\infty} \frac{N_n^{-1} I_1(\alpha_n a) K_1(\alpha_n a)}{(\alpha_n d)^2}, \tag{5.16}$$

where $\nu = \omega^2 d/g$.

20

564 ~~245~~ ~~383~~

We shall now consider the behaviour of these coefficients as $\nu \to 0$. First we shall remind ourselves of the equations satisfied by ν and α_n ($n \geqslant 1$),

$$\nu = kd \tanh kd, \quad \alpha_n d \tan \alpha_n d + \nu = 0, \qquad (5.17), (5.18)$$

and, thus, as $\nu \to 0$ we have $\nu \to (kd)^2$ and $\alpha_n \to n\pi$.

Using the limiting forms of J_1, Y_1 for small arguments (Abramowitz & Stegun 1970), we have the following behaviour of μ and λ as $\nu \to 0$,

$$\lambda \to \pi/4(a/d)^2, \qquad (5.19)$$

$$\mu \to 1 - \frac{4}{\pi^3} \sum_{n=1}^{\infty} I_1(n\pi a/d) K_1(n\pi a/d)/n^2. \qquad (5.20)$$

Both λ and μ tend to finite values as $\nu \to 0$, the series appearing in μ converging fairly rapidly since $I_1(z) K_1(z) \sim \frac{1}{2}z^{-1}$ as $z \to \infty$. As usual, the absorption length will tend to zero as $\nu \to 0$ but the amplitude ratio will tend to a finite value. We have, as $\nu \to 0$, from (4.23) and (5.20) above,

$$\left|\frac{\xi}{A}\right| \to \frac{1}{(\mu_0 \nu_0)}. \qquad (5.21)$$

Now as $\nu \to \infty$,

$$\nu \sim kd \quad \text{and} \quad \alpha_n d \sim n\pi/2, \quad n = 1, 2, \ldots.$$

Thus, we have

$$\mu \to 1 - \frac{16}{\pi^3} \sum_{n=1}^{\infty} I_1\left(\frac{n\pi a}{2d}\right) K_1\left(\frac{n\pi a}{2d}\right) \Big/ n^2. \qquad (5.22)$$

Again μ incorporates a quickly converging series and tends to a finite value.

5.4. *Verification of b_2 result for disk*

Haskind (1957) and Newman (1962) have shown that the damping coefficient is related to the 'exciting force' i.e. the force on the body when it is held fixed in the presence of incoming waves. In this case evaluation of the exciting force is straightforward as there are no diffracted waves. It can be shown from (B 16) and (B 20) that

$$b_2 = \frac{k}{4\rho g c_g |A|^2} |F|^2, \qquad (5.23)$$

where F is the exciting force on the disk, c_g is the group velocity and A is the amplitude of the incoming waves. Now F can be found by integrating the hydrodynamic pressure over the piston surface when the piston is held fixed in incident waves, thus

$$F = -i\omega\rho \int_{\mathscr{S}} \phi_s \, ds \, e^{-i\omega t}, \qquad (5.24)$$

where $\Phi_s = \mathrm{Re}\{\phi_s e^{-i\omega t}\}$ is the scattering potential. This is just the incident wave potential as there are no diffracted waves. Hence

$$\phi_s = \frac{gA}{\omega} \frac{\cosh kz}{\cosh kd} e^{ikx} \qquad (5.25)$$

(taking waves incident from $x = -\infty$ since direction is of no consequence here).

21

365 ~~244~~
~~384~~

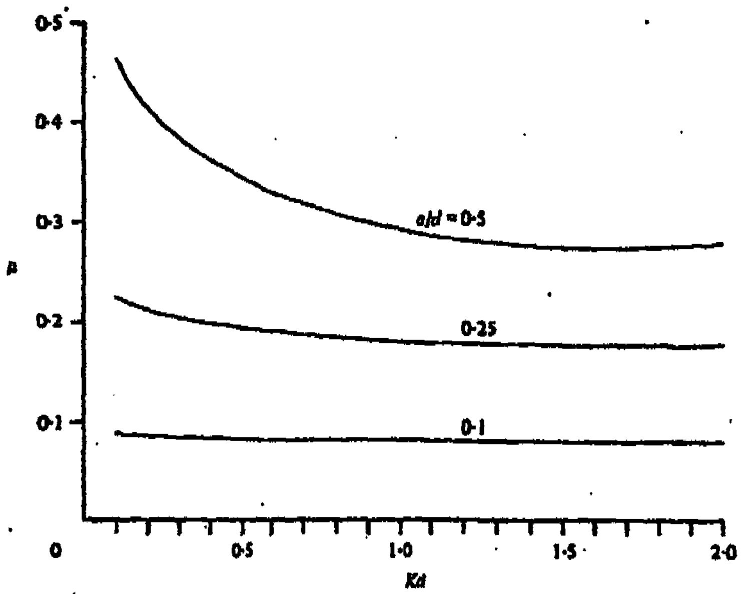

FIGURE 2. Non-dimensional added-mass coefficient β vs. non-dimensional wavenumber Kd, for the disk, for different values of a/d.

Thus

$$F = -i\omega\rho \int_{r=0}^{a} \int_{\theta=0}^{2\pi} \phi_s \Big|_{z=0} r\,dr\,d\theta\, e^{-i\omega t} \tag{5.26}$$

$$= \frac{-i\rho g A}{\cosh kd} \int_0^a r\,dr \int_0^{2\pi} e^{ikr\cos\theta}\, d\theta\, e^{-i\omega t}, \tag{5.27}$$

$$= \frac{-i\rho g A}{\cosh kd} \int_0^a 2\pi r J_0(kr)\, dr\, e^{-i\omega t} \tag{5.28}$$

$$= \frac{-2\pi i\rho g a A}{k \cosh kd} J_1(ka)\, e^{-i\omega t}, \tag{5.29}$$

and, substituting for F in (5.23),

$$b_3 = \frac{\pi^3 a\rho g}{k c_g \cosh^2 kd} J_1^2(ka). \tag{5.30}$$

Now, from (2.10), c_g may be written as

$$c_g = \frac{gkd}{\omega \cosh^2 kd} N_0, \tag{5.31}$$

and, substituting for c_g in (5.30) using (5.31), it can be seen that the expression for b_3 agrees with that obtained from the radiation problem given by (5.12).

560 ~~245~~ 388

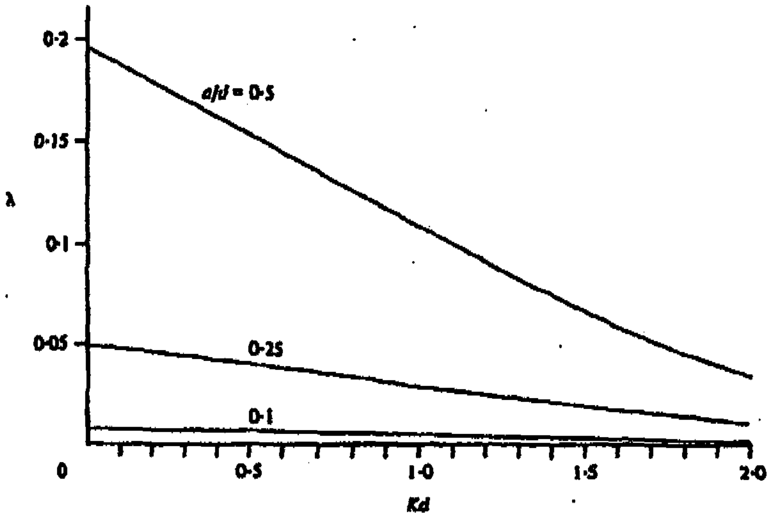

FIGURE 3. Non-dimensional damping coefficient λ vs. non-dimensional wavenumber Kd, for the disk, for different values of a/d.

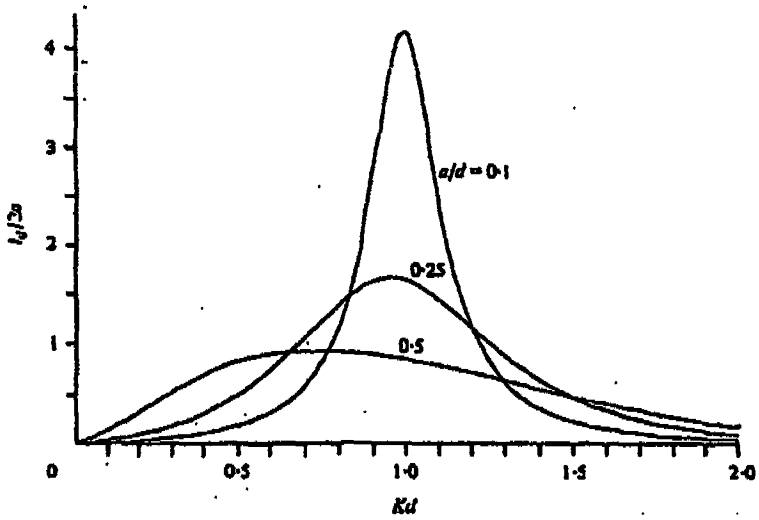

FIGURE 4. Non-dimensional absorption length $l_a/2a$ vs. non-dimensional wavenumber Kd, for the disk, for different values of a/d.

23

567 246 386

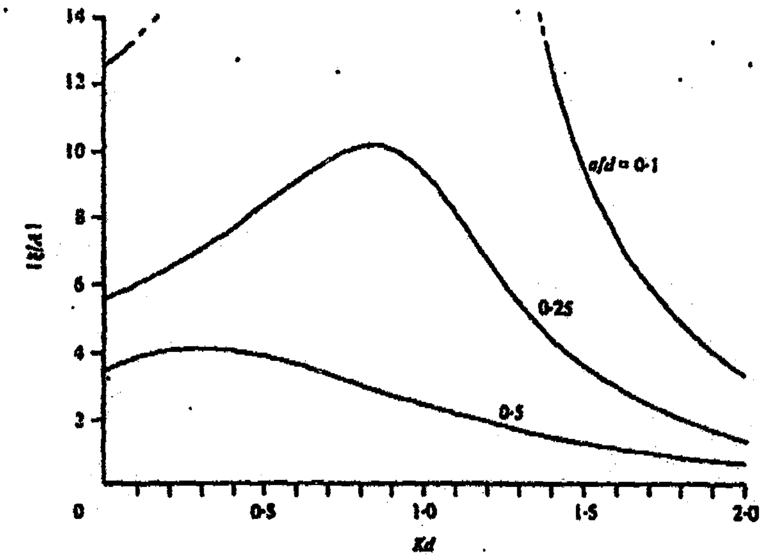

FIGURE 5. Non-dimensional amplitude ratio $|\xi/A|$ *vs.* non-dimensional wavenumber Kd, for the disk, for different values of a/d.

6. Results and discussion

We shall first examine the results for the disk and then proceed with a study of the duct results.

6.1. *The disk on the sea bed*

In each case the results for the disk were plotted for values of $a/d = 0{\cdot}1$, $0{\cdot}25$, $0{\cdot}5$. Figure 2 indicates that, as a/d decreases, so the added-mass variation decreases over the range of ν, and for $a/d = 0{\cdot}1$ the added mass is fairly constant over the whole range. For $a/d = 0{\cdot}5$ the curve begins to rise again slightly near $\nu = 2{\cdot}0$ as the predicted asymptotic value is approached. The damping curves shown in figure 3 illustrate the decrease of the damping coefficient from its asymptotic value at $\nu = 0$ until it reaches its first zero which will occur at a value of $\nu > 2$, when $J_1(ka) = 0$.

We now tune the disk to $\nu_0 = 1{\cdot}0$ as in §4, and the results are shown in figure 4. For the disk to be a good absorber we require $l_d/2a > 1$ over some appreciable range of values of ν. Physically this means that the disk captures all the power in a wave of crest length greater than the disk diameter. Now $l_{d\,\max}/2a = (2ka)^{-1}$ so it would seem that, at the tuned wavenumber, we require $kd < \frac{1}{2}(d/a)$. However, as explained in Srokosz (1979), $l_d/2a$ does not attain its maximum value at ν_0, but to the left of ν_0. This can be most easily seen when $a/d = 0{\cdot}5$ in figure 4 and occurs because, although $l_d/2a < (2ka)^{-1}$ for $\nu \neq \nu_0$, $l_d/2a$ is still able to rise above its value at ν_0 and lie below the curve given by $l_{d\,\max}/2a = (2ka)^{-1}$.

While the curve for $a/d = 0{\cdot}25$, in particular, seems promising, the amplitude ratio curves shown in figure 5 indicate that the disk oscillations are too large to satisfy the assumption of small amplitude motion required in the linear theory. The magnitude

24

568 ~~247~~ ~~387~~

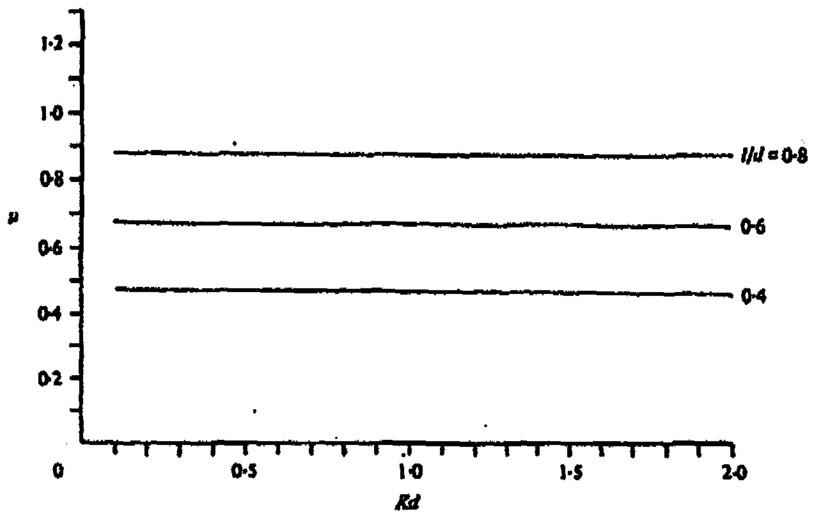

FIGURE 6. Non-dimensional added-mass coefficient μ vs. non-dimensional wave-number Kd, for the duct with $a/d = 0{\cdot}1$, for different values of l/d.

of these oscillations can be reduced by tuning to smaller wavelengths or increasing the disk diameter, however it is not possible to combine these to make the disk a good absorber while ensuring the motion remains within the bounds of linear theory. So, as expected, the disk is not a good absorber and, indeed, the main purpose of its study was to provide a check for the duct results and to provide analytic expressions for the added-mass and damping coefficients, which in many cases behave similarly to those for the duct.

6.2. *The mouth-upward duct*

Figure 6 gives the added-mass curves for fixed $a/d = 0{\cdot}1$ when $l/d = 0{\cdot}4, 0{\cdot}6, 0{\cdot}8$. As for the disk with $a/d = 0{\cdot}1$, the added mass remains fairly constant over the range of ν, and, in each case, the values of the added mass are slightly larger than the mass of water in the tube. This is since, as a/d gets smaller, the piston is effectively having to move the slug of water in the tube and hence the added mass will approach the mass of water in the tube. (We would expect also an end correction L, as in the case of an open pipe in an infinite fluid with no free surfaces present, where $L = 0{\cdot}6133a$. However, this value of L will not apply here due to the pressure of the free surface and sea bed.) The damping curves given in figure 7 show some difference from those for the disk case for larger values of l/d, where the damping now rises to a maximum before decreasing to the first zero. (The zeros of the damping were found to occur at the same values that were obtained for the disk: it is not clear why this is so.)

The added-mass and damping curves for fixed $l/d = 0{\cdot}5$ are shown in figures 8 and 9. Again, the larger variation in the added mass occurs for the wider duct. The damping in each case, although seeming to approach the same value as that for the disk of the same a/d, as $\nu \to 0$, does not fall off as rapidly as that of the disk as ν increases. Before examining the absorption length and amplitude ratio variation with wave-

25

569 ~~248~~ ~~388~~

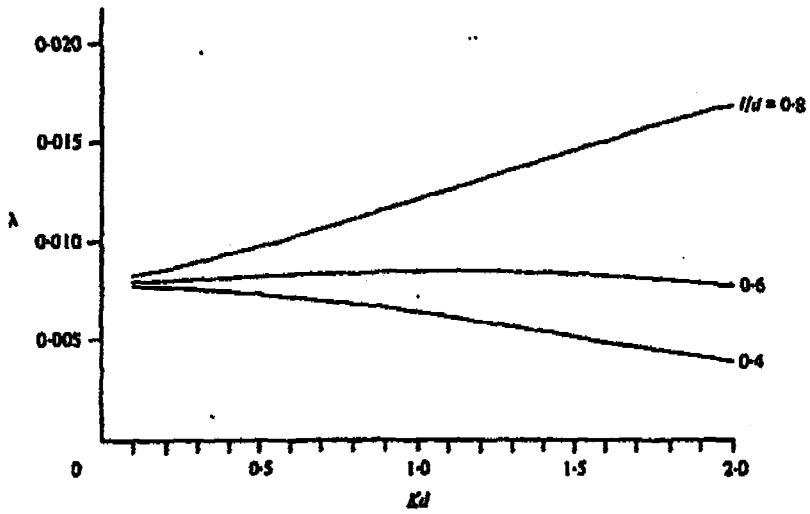

FIGURE 7. Non-dimensional damping coefficient λ *vs.* non-dimensional wavenumber Kd, for the duct with $a/d = 0·1$, for different values of l/d.

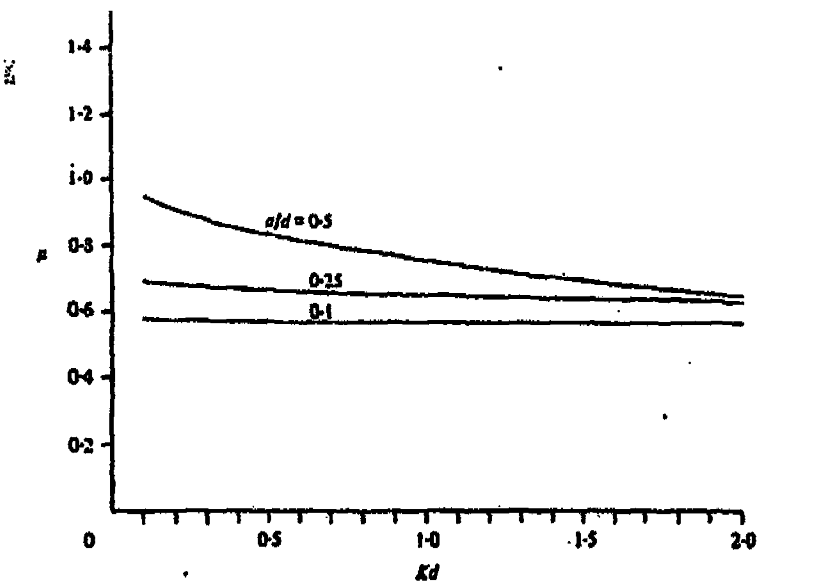

FIGURE 8. Non-dimensional added-mass coefficient μ *vs.* non-dimensional wavenumber Kd, for the duct with $l/d = 0·5$, for different values of a/d.

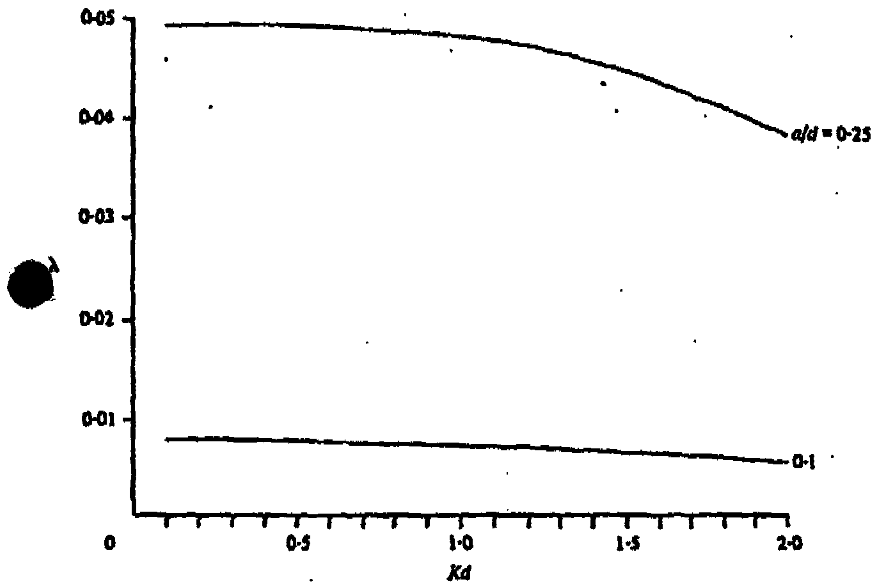

FIGURE 9. Non-dimensional damping coefficient λ *vs.* non-dimensional wavenumber Kd, for the duct with $l/d = 0\cdot5$, for different values of a/d.

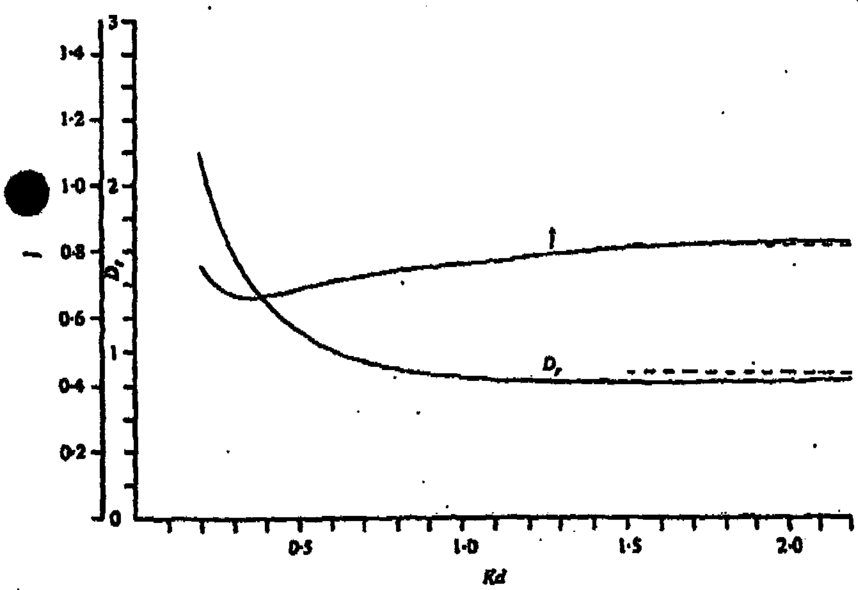

FIGURE 10. Comparison of results for added length $\hat{l}$, and damping coefficient D_r *vs.* non-dimensional wavenumber Kd, with Simon (1981) for $Ka = 0\cdot2$, $Kh = 0\cdot2$. – – –, Simon's results in infinite depth; ——, results in finite depth.

570 ~~249~~ ~~389~~

27

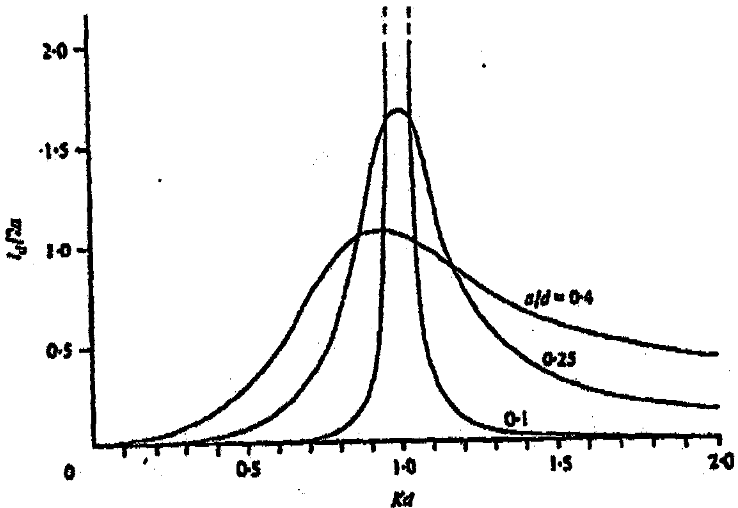

FIGURE 11. Non-dimensional absorption length $l_a/2a$ vs. non-dimensional wavenumber Kd, for the duct with $l/d = 0{\cdot}8$, $\nu_0 = 1{\cdot}0$, for different values of a/d.

number we shall study the behaviour of the added-mass and damping coefficients as the depth increases. By fixing ω^2a/g, ω^2h/g and plotting the added mass and damping as functions of ω^2d/g we should recover the infinite depth results of Simon (1981) as $\omega^2d/g \to \infty$. However, it is first necessary to relate the damping and added mass to the damping coefficient, D_r, and the effective added-length term, $\hat{l}$, used by Simon. This can be done by examining the respective radiation problems. In the model used here, a piston displacement $\mathrm{Re}[\xi e^{-i\omega t}]$ radiates energy away at a rate $\frac{1}{2}\omega^2 b_3|\xi|^2$ while, in the radiation problem set up by Simon, a volume flow $\mathrm{Re}[Qe^{i\omega t}]$ in the duct radiates energy away at a rate $\frac{1}{2}\rho\omega K D_r|Q|^2$ (Simon 1981). If we define $D_r, \hat{l}$ in finite depth such that they correspond to $D_r, \hat{l}$ defined in infinite depth by Simon, then after some algebra we find

$$\lambda = \frac{\pi}{2}\left(\frac{a}{d}\right)\left(\frac{\omega^2 a}{g}\right)D_r, \quad \mu = \left(\frac{a}{d}\right)\left\{\frac{l}{a}+\hat{l}\right\}. \qquad (6.1),\ (6.2)$$

Now, using this definition of $D_r, \hat{l}$, we should recover the infinite depth values as $\omega^2d/g \to \infty$. Figure 10 gives the variation of D_r and $\hat{l}$ with ω^2d/g, when $\omega^2a/g = \omega^2h/g = 0{\cdot}2$. In all cases, the values seem to be converging to the infinite depth values of Simon (1981). The accuracy of the results decreases as ω^2d/g increases and so, for $\omega^2a/g = 0{\cdot}2$, it is not possible to be confident about results for $\omega^2d/g > 2$ say. Note that D_r approaches its infinite depth value from below, although, for $\omega^2d/g < 0{\cdot}8$, D_r is greater than its infinite depth value.

Figure 11 shows the absorption length variation for fixed $l/d = 0{\cdot}8$, with tuned wavenumber once more $\nu_0 = 1{\cdot}0$. It can be seen that widening the duct diameter will broaden the curve. The same criterion as for the disk applies in determining whether the device is a good absorber; i.e. as a guide we require $kd < \frac{1}{2}(d/a)$ at the tuned wavenumber. So, although the duct could be better tuned, in the case $a/d = 0{\cdot}1$ say, 592 25/391

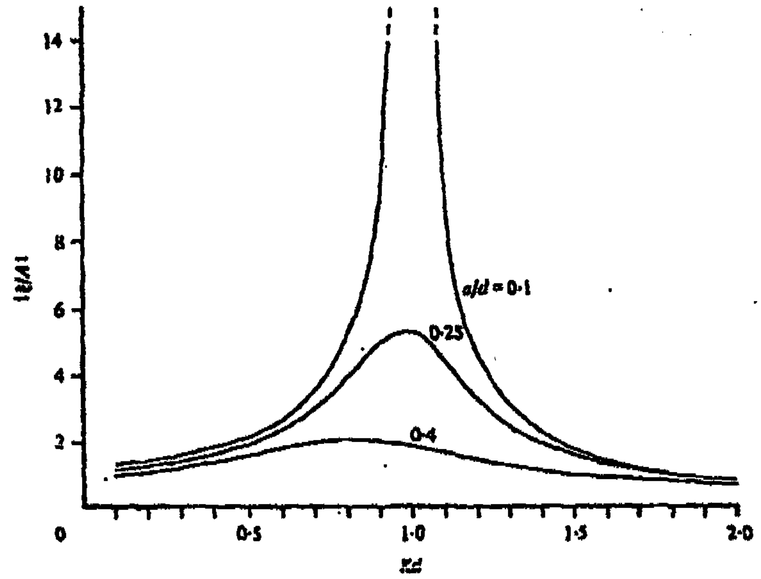

FIGURE 12. Non-dimensional amplitude ratio $|\xi/A|$ *vs.* non-dimensional wavenumber Kd, for the duct with $l/d = 0{\cdot}8$, $\nu_0 = 1{\cdot}0$, *for different values of* a/d.

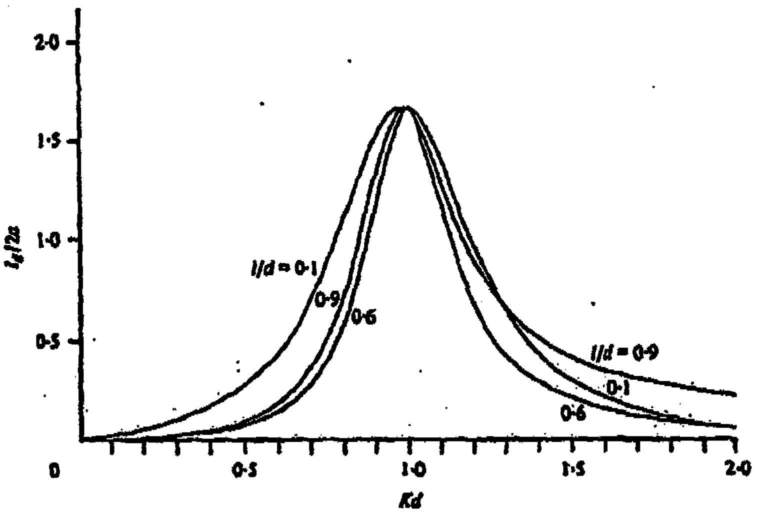

FIGURE 13. Non-dimensional absorption length $l_e/2a$ *vs.* non-dimensional wavenumber Kd, for the duct with $a/d = 0{\cdot}25$, $\nu_0 = 1{\cdot}0$, *for different values of* l/d.

29

573 28 392

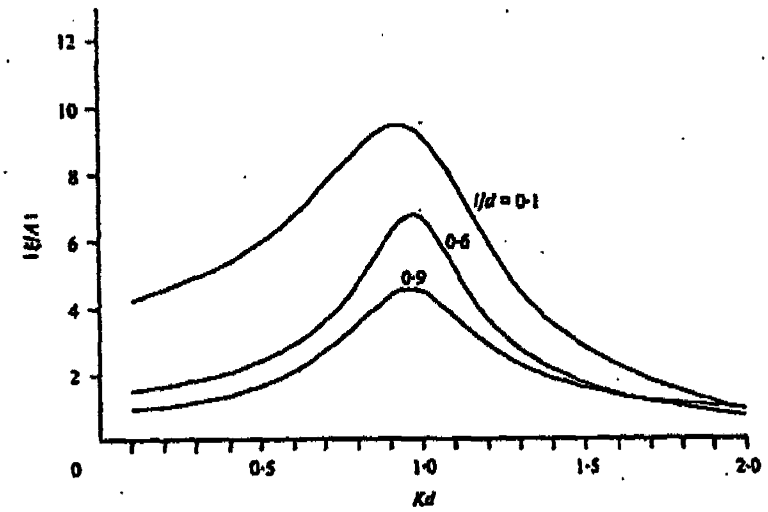

FIGURE 14. Non-dimensional amplitude ratio $|\xi/A|$ *vs.* non-dimensional wavenumber Kd, for the duct with $a/d = 0{\cdot}25$, $\nu_s = 1{\cdot}0$, for different values of l/d.

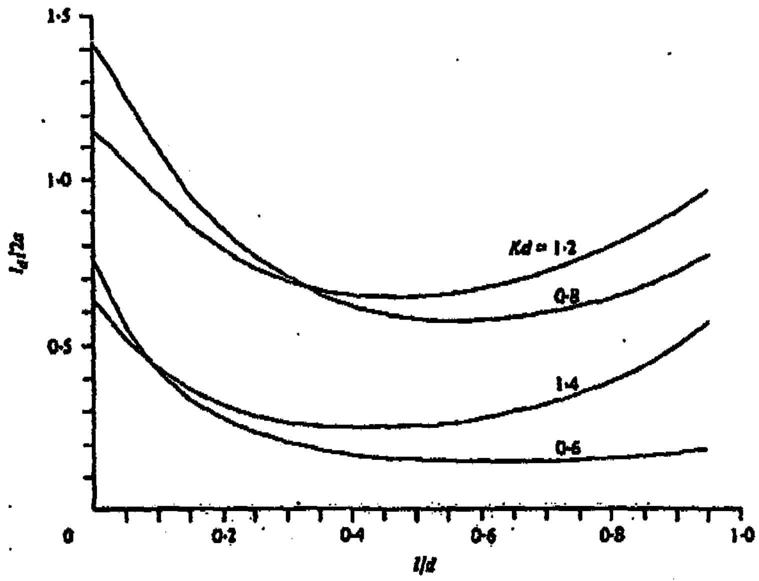

FIGURE 15. Non-dimensional absorption length $l_a/2a$ *vs.* l/d with $a/d = 0{\cdot}25$, $\nu_s = 1{\cdot}0$, for different values of Kd.

30

574 ~~253~~ ~~393~~

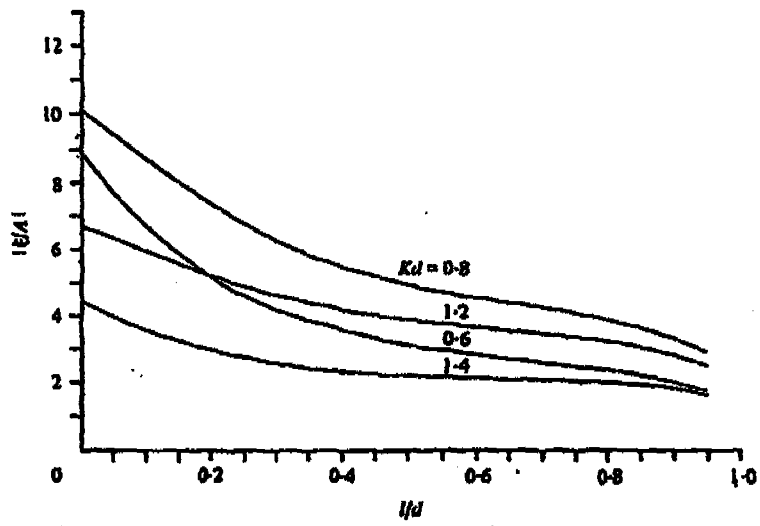

FIGURE 16. Non-dimensional amplitude ratio $|\xi/A|$ *vs.* l/d with $a/d = 0.25$, $\nu_0 = 1.0$, for different values of Kd.

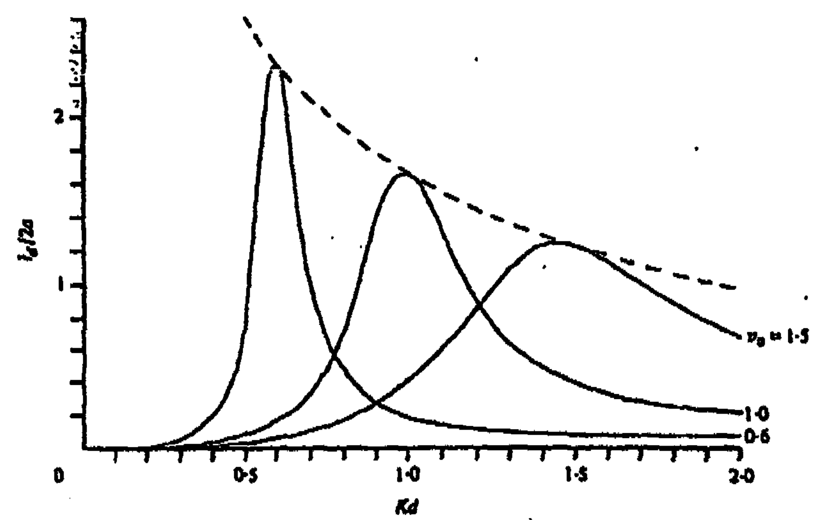

FIGURE 17. Non-dimensional absorption length $l_a/2a$ *vs.* non-dimensional wavenumber Kd, with $a/d = 0.25$; $l/d = 0.9$ for different values of tuned wavenumber ν_0. The dashed curve represents the maximum absorption length, $l_{a_{max}}/2a$.

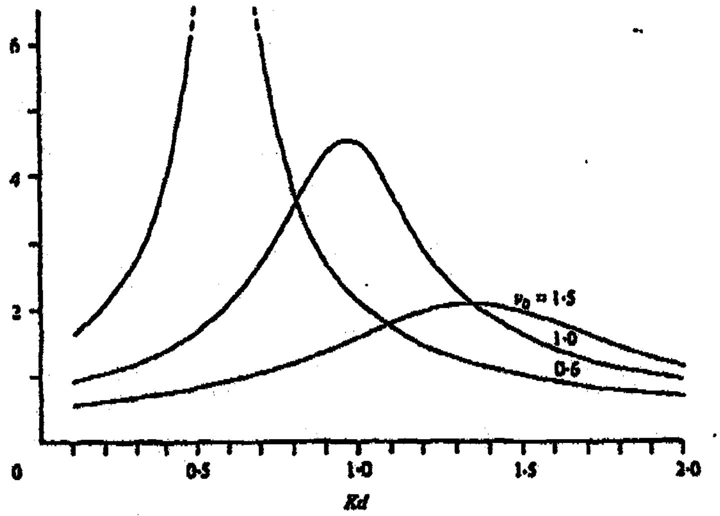

FIGURE 13. Non-dimensional amplitude ratio $|\xi/A|$ *vs.* non-dimensional wavenumber Kd, with $a/d = 0·25$, $l/d = 0·9$ for different values of tuned wavenumber ν_0.

figure 12 indicates that the duct diameter should perhaps be too large in order that the assumptions of linear theory be satisfied.

If we now study the absorption length at fixed a/d and vary l/d, the results are not quite so straightforward. As one might expect, figure 13 shows that a wider bandwidth is achieved for $l/d = 0·9$ rather than 0·6, when the duct mouth is closer to the surface. But when $l/d = 0·1$ the bandwidth is wider than in the previous two cases, although the curve does drop off quicker than the curve corresponding to $l/d = 0·9$, as ν increases. On the other hand, the amplitude ratios shown in figure 14 indicate a progressive decrease in $|\xi/A|$ as l/d increases, over practically the whole range, and certainly near the tuned wavenumber. To understand further what is happening here, attention was focused on a fixed value of ν and the variation of absorption length with l/d was studied (figure 15).

Surprisingly, as l/d increases from zero, the bandwidth of the absorption length curve decreases before reaching a minimum and then increases as the duct mouth gets close to the surface. From figure 16 it can be seen that the amplitude ratio falls off rapidly at first before levelling off to some extent until the mouth becomes close to the surface, when it begins to fall again. Apparently, the advantage of the duct is to decrease the amplitude ratio considerably but the tube, in some sense, shields the piston from the incident wave train, although this may be offset by having the duct mouth near the surface.

The effect of tuning to different wavenumbers may be seen in figure 17. The maximum value of $l_a/2a$ is given by the curve $l_{a\,\max}/2a = (2ka)^{-1}$, shown dotted. Figure 18 shows how the piston oscillations are reduced as ν_0 increases. When $\nu_0 = 0·6$ the absorption length bandwidth is very narrow and the amplitude ratio rises markedly

575 214 394

32

above the values where linear theory is applicable. But, when $\nu_0 = 1 \cdot 5$, the amplitude ratio is greatly reduced, as noted in §6.1, linear theory is valid, and the absorption width curve exhibits a broad bandwidth.

6.3. *A note on numerical methods*

We require the solution of two infinite systems of real equations. This was obtained by truncating the systems after N terms and solving the finite system using a standard numerical procedure. Both systems have the same left-hand sides so the matrix of coefficients of e_n, δ_n need only be inverted once numerically. Then, regarding the solutions obtained as functions of N, we require the limit as $N \to \infty$. By plotting the results against N^{-1} and extrapolating to zero, we may study the convergence of the solutions.

The convergence is slow, being almost linearly dependent on $1/N$ for large N, as Garrett (1970) noted. The equations were solved with $N = 10$, in steps of 10, up to $N = 80$ terms. Unlike Garrett, the solution for $N = 40$ was accurate to within 1% and a linear extrapolation using $N = 40$, 50 compared well with a smooth extrapolation through all the values of N. Using this linear extrapolation, agreement was found to three or four significant figures in general. For smaller values of a/d and certain values of ν, N needs to be larger to maintain the accuracy.

7. Conclusion

In this paper a simplified model of an oscillating water column wave-energy absorber has been used to study the behaviour of the added-mass and damping coefficients and, hence, the absorption length. Expressions for the absorption length and amplitude ratio corresponding to those of Evans (1976) were derived for finite depth, for a general axisymmetric heaving body. The limiting case of an oscillating disk on the sea bed was also analysed, and while this is not a practical device it provided some insight into the behaviour of the added-mass and damping coefficients as well as providing a useful check on the numerical methods used in the duct problem.

The results indicate that, unless a/d is large, the added mass shows relatively little change over the range of ν, while the damping coefficient still retains the zeros found in the disk problem, although the presence of the duct can greatly modify the curves. The added-mass and damping behaviour with increasing depth is presented, showing how these coefficients approach the infinite depth value of Simon (1981).

The variation of absorption length with wavenumber has been illustrated for both fixed a/d and fixed l/d. An unexpected result was that increasing the tube length can actually narrow the bandwidth of the curves. For moderate values of l/d and $2a/d$ the linear theory is not really applicable and, although the amplitude ratio may be reduced, to some extent, by choosing more appropriate tuning wavenumbers, for the device to be a good absorber it is necessary for l/d and $2a/d$ to be quite large, $l/d = 0 \cdot 9$, $a/d = 0 \cdot 4$ say.

Thus, such a device situated on the sea bed does not seem practical and better results may be obtained by bringing the device closer to the sea surface. However, it must be pointed out that devices of this type will not be isolated but will appear in arrays where interaction effects can occur which may result in an increase in absorption width.

I would like to thank Dr D. V. Evans for many helpful discussions during the course of this work and the Science Research Council for providing the financial support.

Appendix A

We have

$$D_{mn} = \frac{1}{d}\int_l^d Z_m(z)\,Z_n(z)\,dz, \tag{A 1}$$

giving

$$D_{mn} = (N_n N_m)^{-\frac{1}{2}}\,[\alpha_n d \sin \alpha_n l \cos \alpha_m l - \alpha_m d \sin \alpha_m l \cos \alpha_n l]/(\alpha_m^2 d^2 - \alpha_n^2 d^2) \tag{A 2}$$

for $m \neq n$, $m, n \geqslant 1$;

$$D_{mm} = \frac{1}{2}\frac{h}{d} N_m^{-1}\left[1 + \frac{\sin \alpha_m h \cos \alpha_m (l+d)}{\alpha_m h}\right] \tag{A 3}$$

for $m \geqslant 1$;

$$D_{0n} = D_{n0} = -(N_0 N_n)^{-\frac{1}{2}}\,[kd \sinh kl \cos \alpha_n l + \alpha_n d \cosh kl \sin \alpha_n l]/(\alpha_n^2 d^2 + k^2 d^2) \tag{A 4}$$

for $n \geqslant 1$;

$$D_{00} = \frac{1}{2}\frac{h}{d} N_0^{-1}\left[1 + \frac{\sinh kh \cosh k(l+d)}{kh}\right]. \tag{A 5}$$

Now

$$C_m = \frac{1}{ad}\int_l^d [(d-z) - g/\omega^2]\,Z_m(z)\,dz, \tag{A 6}$$

giving

$$C_0 = -\frac{N_0^{-\frac{1}{2}}}{ka}\left[\frac{\sinh kh}{kd \sinh kd} + \frac{h}{d}\sinh kl\right], \tag{A 7}$$

$$C_m = \frac{N_m^{-\frac{1}{2}}}{\alpha_m a}\left[\frac{\sin \alpha_m h}{\alpha_m d \sin \alpha_m d} - \frac{h}{d}\sin \alpha_m l\right] \tag{A 8}$$

for $m \geqslant 1$.

We have written, in equation (3.7),

$$E_{m0} = \gamma_m + i\beta_m, \tag{A 9}$$

where γ_m, β_m are real, for $m \geqslant 0$; now, from (3.3),

$$E_{m0} = (R_0 - 1)\,D_{m0} + \delta_{m0}. \tag{A 10}$$

Thus

$$\gamma_m = \left[\frac{Y_1(ka)}{\frac{1}{2}\pi k^2 a^2 J_1(ka)}\,(J_1^2(ka) + Y_1^2(ka))^{-1} - 1\right] D_{m0} + \delta_{m0}, \tag{A 11}$$

$$\beta_m = \frac{D_{m0}}{\frac{1}{2}\pi k^2 a^2}\,(J_1^2(ka) + Y_1^2(ka))^{-1}. \tag{A 12}$$

Note: For the disk case, we have $l = 0$, and so

$$C_0 = -\frac{N_0^{-\frac{1}{2}}}{k^2 ad}, \tag{A 13}$$

$$C_m = \frac{N_m^{-\frac{1}{2}}}{\alpha_m^2 ad}. \tag{A 14}$$

578 257
39

Appendix B

Absorption width in finite depth. Consider the full problem of waves incident upon the duct. The equation of motion of the piston is

$$m\ddot{\zeta}+\bar{d}\dot{\zeta}+\bar{k}\zeta = F_T, \tag{B 1}$$

where $\bar{k}, \bar{d}$ are the spring and damper constants respectively, F_T is the hydrodynamical force on the piston, and

$$\zeta = \mathrm{Re}\{\xi e^{-i\omega t}\} \tag{B 2}$$

is the displacement of the piston.

Now

$$F_T = F_d + F_r \tag{B 3}$$

where F_d is the force on the piston when it is held fixed in the presence of incoming waves (the scattering problem), and F_r is the force on the piston when it is oscillating with displacement ζ in the absence of incoming waves (a radiation problem).

And, by definition,

$$F_r = f_{33}\xi e^{-i\omega t} \quad \text{(real part understood)}, \tag{B 4}$$

where f_{33} is defined in equation (4.1), i.e.

$$F_r = (\omega^2 a_3 + i\omega b_3)\xi e^{-i\omega t}. \tag{B 5}$$

Substituting in equation (B 1) we obtain

$$F_d = \mathrm{Re}\{[(\bar{k}-(m+a_3)\omega^2) - i\omega(\bar{d}+b_3)]\xi e^{-i\omega t}\}. \tag{B 6}$$

To calculate F_d. The Haskind relations show that the exciting force depends only on the far-field potential of the radiation potential, and is given by

$$F_d = i\omega\rho e^{-i\omega t}\int_{\mathscr{S}_0}\left(\phi_0\frac{\partial\phi}{\partial n} - \phi\frac{\partial\phi_0}{\partial n}\right)dS, \tag{B 7}$$

where $\Phi = \mathrm{Re}\{\phi e^{-i\omega t}\}$ is the radiation potential, defined as in §2, and $\mathscr{S}_0$ is a control surface, a cylindrical surface, $r = R$ (excluding base and top), with normal directed towards the origin. The incident wave potential is given by $\Phi_0 = \mathrm{Re}\{\phi_0 e^{-i\omega t}\}$, where

$$\phi_0 = \frac{gA}{\omega}\frac{\cosh kz}{\cosh kd}e^{ikx}, \tag{B 8}$$

representing a wave of amplitude $|A|$, wavenumber k, in water of finite depth d, and this may be written

$$\phi_0 = \frac{gA}{\omega}\frac{\cosh kz}{\cosh kd}\sum_{m=0}^{\infty}\epsilon_m i^m J_m(kr)\cos m\theta \tag{B 9}$$

$$= \frac{gA}{\omega}\frac{\cosh kz}{\cosh kd}\sum_{m=0}^{\infty}\frac{\epsilon_m i^m}{2}[H_m^{(1)}(kr)+H_m^{(2)}(kr)], \tag{B 10}$$

where $\epsilon_0 = 1$, $\epsilon_m = 2$ $(m \geqslant 1)$, and $H_m^{(1)}$, $H_m^{(2)}$ are Hankel functions of the first and second kinds respectively.

As $r \to \infty$, the radiation condition imposed on ϕ gives

$$\phi \sim A_r H_0^{(1)}(kr)\frac{\cosh kz}{\cosh kd}, \tag{B 11}$$

where A_r is some (complex) constant.

35

So taking $r = R$ as control surface and letting $R \to \infty$, the expression for F_d reduces to

$$F_d = -\frac{\pi i \rho g k A A_r e^{-i\omega t}}{\cosh^2 kd} \int_0^d \cosh^2 kz\, dz \lim_{R\to\infty} R[H_0^{(1)}(kr)\, H_1^{(2)}(kr) - H_0^{(2)}(kr)\, H_1^{(1)}(kr)]. \quad \text{(B 12)}$$

Thus

$$F_d = -\frac{i\rho g k A A_r}{\cosh^2 kd} N_0 d \frac{4i}{k} e^{-i\omega t}, \quad \text{(B 13)}$$

where use has been made of the asymptotic forms of the Hankel functions for large arguments (Abramowitz & Stegun 1970).

Therefore

$$F_d = \frac{4\rho g d N_0 A A_r}{\cosh^2 kd} e^{-i\omega t}, \quad \text{(B 14)}$$

or

$$F_d = 4\rho A A_r c_g \frac{\omega}{k} e^{-i\omega t}, \quad \text{(B 15)}$$

where c_g is the group velocity in depth d.

Now, applying Green's theorem to ϕ and $\bar{\phi}$ ($\bar{\phi}$ represents the complex conjugate of ϕ), it can be shown that

$$\frac{2i}{\rho\omega} b_3 = \int_{\mathscr{S}_0} \left(\phi \frac{\partial \bar{\phi}}{\partial n} - \bar{\phi} \frac{\partial \phi}{\partial n}\right) dS, \quad \text{(B 16)}$$

where $\mathscr{S}_0$ is the control surface previously defined and, as $R \to \infty$,

$$\phi \sim A_r H_0^{(1)}(kR) \frac{\cosh kz}{\cosh kd}, \quad \text{(B 17)}$$

$$\bar{\phi} \sim A_r H_0^{(2)}(kR) \frac{\cosh kz}{\cosh kd}, \quad \text{(B 18)}$$

and, substituting for ϕ, $\bar{\phi}$, (B 16) reduces to

$$b_3 = \frac{4\rho\omega d N_0}{\cosh^2 kd} |A_r|^2 \quad \text{(B 19)}$$

$$= \frac{4\rho}{gk} c_g \omega^2 |A_r|^2. \quad \text{(B 20)}$$

If we use the expression for F_d in (B 15), (B 6) becomes

$$\frac{4\rho\omega c_g}{k} A A_r = [(\bar{k} - (m + a_3)\omega^2) - i\omega(\bar{d} + b_3)]\,\xi. \quad \text{(B 21)}$$

The power absorbed by the system is the mean rate at which work is done on the system by the fluid,

$$P = \frac{\omega}{2\pi} \int_0^{2\pi/\omega} \dot{\xi} F_T\, dt = \tfrac{1}{2}\omega^2 \bar{d} |\xi|^2, \quad \text{(B 22)}$$

and the power per unit frontage of the incident wave is

$$P_0 = (\text{wave energy density}) \times (\text{group velocity})$$
$$= \tfrac{1}{2}\rho g |A|^2 c_g. \quad \text{(B 23)}$$

Hence the absorption width l_a is given by

$$l_a = \frac{P}{P_0} \tag{B 24}$$

$$= \frac{\omega^2}{\rho g c_g} \bar{d} \left|\frac{\xi}{A}\right|^2. \tag{B 25}$$

Substituting for $|\xi/A|$ from (B 21) and using (B 20) to eliminate $|A_r|$, this becomes

$$l_a = \frac{4(\omega^2/k) b_3 \bar{d}}{[(\bar{k}-(m+a_3)\omega^2)^2+\omega^2(\bar{d}+b_3)^2]}. \tag{B 26}$$

Note that for deep water we have $\omega^2 = gk$ and the deep water result is obtained (Evans 1976).

REFERENCES

Abramowitz, M. & Stegun, I. A. 1970 *Handbook of Mathematical Functions* 9th edn. Dover Publications.

Black, J. L., Mei, C. C. & Bray, M. C. G. 1971 Radiation and scattering of water waves by rigid bodies. *J. Fluid Mech.* 46, 151–164.

Evans, D. V. 1976 A theory for wave-power absorption by oscillating bodies. *J. Fluid Mech.* 77, 1–25.

Garrett, C. J. R. 1970 Bottomless harbours. *J. Fluid Mech.* 43, 433–449.

Garrett, C. J. R. 1971 Wave forces on a circular dock. *J. Fluid Mech.* 46, 129–139.

Haskind, M. D. 1957 The exciting forces and wetting of ships in waves. *Izv. Akad. Nauk S.S.S.R., Otd. Tekh. Nauk* 7, 65–79. (English trans. *David Taylor, Model Basin Trans.* no. 307.)

Lighthill, J. 1979 Two-dimensional analyses related to wave-energy extraction by submerged resonant ducts. *J. Fluid Mech.* 91, 253–317.

Miles, J. W. & Gilbert, F. 1968 Scattering of gravity waves by a circular dock. *J. Fluid Mech.* 34, 783–793.

Newman, J. N. 1962 The exciting forces on fixed bodies in waves. *J. Ship Res.* 6, 10–17.

Newman, J. N. 1977 *Marine Hydrodynamics*. Massachusetts Institute of Technology Press.

Ogilvie, T. F. 1963 First- and second-order forces on a cylinder submerged under a free surface. *J. Fluid Mech.* 16, 451–472.

Simon, M. 1981 Wave-energy extraction by a submerged cylindrical resonant duct. *J. Fluid Mech.* 104, 159–187.

Srokosz, M. A. 1979 The submerged sphere as an absorber of wave power. *J. Fluid Mech.* 95, 717–741.

399 580

37

SUPERINTENDENCIA DE INDUSTRIA Y COMERCIO
DIVISION DE NUEVAS CREACIONES

Radicación No. 05-44485
Clasificación Internacional (IPC): F03B 13/18
Concepto Técnico No. 2246

Patente de Invención	☐		
Vía PCT (fase nacional)	☐	Cap. II	☐
No. Sol. Internacional	PCT/US2003/032377		
Publicación Internacional	WO 2004/033900		

Como resultado del examen definitivo, realizado con fundamento en el artículo 48 de la Decisión 486 de la Comisión de la Comunidad Andina, se le comunica:

1. **Documentos estudiados**

1.1. <u>Descripción</u>:	Folios **77 a 186,** presentada originalmente.
1.2. <u>Reivindicaciones</u>:	28, folios **326 a 345,** respuesta examen fondo.
1.3. <u>Dibujos</u>:	**17** figuras, folios **346 a 362.**
1.4. <u>Prioridad</u>:	US 60/417/914 de 2002/10/10.
1.5. <u>Oposiciones</u>:	No se presentaron oposiciones a la solicitud.

2. **Objeto de la invención**

- Título de la solicitud: *Bomba hidrostática.*
- Nuevo título de la solicitud: ***Bomba hidrostática de pistón con bloque flotante.*** Se cambia de oficio, por ajustarse con precisión al objeto de la solicitud.
- *El objeto de la invención es una bomba hidrostática de pistón anclada al piso marino, que aprovecha la energía potencial de las olas.*
- *La solicitud de modelo de utilidad se catalogó, según la Clasificación Internacional de Patentes (IPC.) en:* ***F03B 13/18.***

3. **De la solicitud de Patente** (según el caso)

3.1. Descripción *(artículo 28 D. 486)*

- *La descripción sí cumple con el requisito de claridad o comprensión de acuerdo al art. 28 de la Decisión 486.*

901
582

3.2. Reivindicaciones *(artículo 30 D 486)*

- *Las reivindicaciones sí cumplen con el requisito de claridad, concisión o sustento por la descripción de acuerdo al art. 30 de la Decisión 486.*

4. **Unidad de invención** *(artículo 25 D 486)*

- *El capítulo reivindicatorio sí cumple con el requisito de unidad de invención.*

5. **No es una invención** *(artículo 15 D 486 literal a)-f))* (según causal)

- *Las reivindicaciones sí son patentables.*

6. **Excepción a la patentabilidad** *(artículo 20 D486 literal a)-d))* (según causal)

- *Las reivindicaciones presentadas sí son patentables.*

7. **Reivindicaciones relativas a un uso o a un uso distinto** *(artículos 14 y 21 D 486)*

- *El objeto de la solicitud sí es un objeto patentable.*

8. **Determinación del Estado de la Técnica**

- *Consultadas las bases de datos con que cuenta la oficina y las otras fuentes utilizadas para determinar el estado de la técnica, antes del* ***10 de octubre de 2002,*** *fecha de la prioridad invocada, no se encontró documento alguno relacionado con el objeto de la solicitud o que afectara su patentabilidad.*

9. **Análisis de patentabilidad (artículo 14 D486)**

9.1. **Novedad** *(artículo 16 D486)*

- *Reivindicación 1: Bomba hidrostática caracterizada porque comprende:*
  - *Un bloque flotante que tiene un volumen ajustable que se puede operar para moverse en forma reciprocante en respuesta a una acción de la ola, y*
  - *Un pistón colocado de manera deslizable dentro de un cilindro del pistón y conectado con el bloque flotante, el pistón se puede hacer mover en forma reciprocante en una dirección y en una segunda dirección en respuesta al movimiento del bloque flotante, el pistón se mueve en la segunda dirección para extraer un fluido de operación en el cilindro del pistón y se mueve en la primera dirección para impulsar el fluido de operación fuera del cilindro del pistón.*

- *Las reivindicaciones 1 a 28, folios 326 a 345, del nuevo capítulo reivindicatorio presentado.*

- *De acuerdo con el numeral 8, no se encontró dentro del estado de la técnica, documento alguno que evidenciara la existencia de la invención.*

- *Por tanto se concluye que las reivindicaciones 1 a 28, son novedosas, de acuerdo a lo estipulado en el art. 16 de la Decisión 486 de la Comisión de la Comunidad Andina.*

9.2. <u>**Nivel inventivo**</u> *(artículo 18 D486)*

- *Para las reivindicaciones 1 a 28, del numeral 9.1., no se encontró dentro del estado de la técnica, tal como lo estipulado en el numeral 8, documento alguno que afecte el nivel inventivo.*

- *Se concluye que tienen nivel inventivo de acuerdo a lo estipulado en el art. 18 de la Decisión 486 de la Comisión de la Comunidad Andina.*

9.3. <u>**Aplicación industrial**</u> *(artículo 19 D 486)*

- *Las reivindicaciones 1 a 28, del punto 9.1., la invención sí tiene Aplicación Industrial, en la industria de bombas hidrostáticas de pistón, con bloque flotante ajustable, bombas ancladas al piso marino que operan con la energía potencial del movimiento de las olas.*

10. Conclusión:

En consecuencia y por todo lo expuesto anteriormente, se recomienda **Conceder** las reivindicaciones: **1 a 28,** folios **326 a 345,** con el nuevo título cambiado por parte de la oficina administradora: ***Bomba hidrostática de pistón con bloque flotante.***

Bogotá, D.C.,

CONCEPTO TECNICO No. 2246	**EXAMINADOR TECNICO** Código No. 202051